

A Full Mission Summary (1997-2017) of the Attitude Control Performance during Orbit Trim Maneuvers Performed by the Cassini-Huygens Spacecraft

Todd S. Brown,¹

Jet Propulsion Laboratory, California Institute of Technology, Pasadena, CA, 91109

The Cassini mission was a highly successful 20-year mission to the planet Saturn that launched in 1997 and concluded its mission in September 2017. Over the course of its mission, Cassini executed hundreds of main engine and thruster-controlled ΔV maneuvers. This paper provides an overview of the Cassini maneuvers and provides data on the performance of the attitude controller and maneuver execution errors during these maneuvers. The paper concludes with an appendix documenting the vital statistics for all maneuvers that Cassini performed.

Acronyms

<i>AACS</i>	=	attitude and articulation control subsystem
<i>AFC</i>	=	attitude control flight computer
<i>CM</i>	=	center of mass
<i>DSM</i>	=	deep space maneuver
<i>DSN</i>	=	deep space network
<i>ESA</i>	=	European Space Agency
<i>FSW</i>	=	flight software
<i>NASA</i>	=	National Aeronautics and Space Administration
<i>HGA</i>	=	high gain antenna
<i>IRU</i>	=	inertial reference unit (gyroscope)
<i>JPL</i>	=	Jet Propulsion Laboratory
<i>JTM</i>	=	backup orbit trim maneuver
<i>ME</i>	=	main engine
<i>NAV</i>	=	navigation team
<i>OTM</i>	=	orbit trim maneuver
<i>PRM</i>	=	periapsis raise maneuver
<i>Prop</i>	=	propulsion
<i>RCS</i>	=	reaction control system
<i>RTG</i>	=	radioisotope thermoelectric generator
<i>RWA</i>	=	reaction wheel assembly
<i>SC</i>	=	spacecraft
<i>SCO</i>	=	spacecraft operations
<i>SOI</i>	=	Saturn orbit insertion
<i>SRU</i>	=	stellar reference unit (star tracker)
<i>TCM</i>	=	trajectory correction maneuver
<i>XM</i>	=	equinox (extended) mission
<i>XXM</i>	=	solstice (extended-extended) mission
ΔV	=	change in spacecraft velocity

¹ Member of Technical Staff, Guidance & Control Spacecraft Systems Engineering Group, Mail Stop 230-104, Jet Propulsion Laboratory, 4800 Oak Grove Drive, Pasadena, California 91109-8099, USA.

I. Introduction

THE Cassini-Huygens Mission was a joint NASA and ESA project to study the planet Saturn and its moons. Cassini was launched aboard a Titan IV rocket from Cape Canaveral on October 15, 1997 to begin a 7-year-long cruise to Saturn that included gravity assist flybys of Venus in 1998 and 1999, Earth (also in 1999), and Jupiter in late 2000, before ultimately arriving at Saturn in June 2004.¹ On December 25, 2004, shortly after the arrival at Saturn, the Cassini spacecraft deployed the ESA Huygens probe, which parachuted to a successful soft landing on Saturn's moon, Titan, in January 2005.² After the Huygens probe was released, the Cassini spacecraft proceeded to perform the Prime Science Mission (2004-2008), the two-year Equinox Extended Mission (2008-2010)³, and the seven-year Solstice Mission (2010-2017).⁴ In April 2017, after 19 years of flight, and as a Grand Finale for the mission, Cassini entered into the Proximal Orbits. These Proximal Orbits were 22 roughly week-long orbits around Saturn that crossed the ring-plane in the narrow gap between the innermost rings of Saturn and the cloud tops of Saturn's atmosphere. This region around Saturn had previously never been explored by any spacecraft. Finally, on September 15, 2017, just one month shy of the 20-year anniversary of launch, the Cassini spacecraft ended its highly successful mission with an intentional fiery destruction via an impact into Saturn's atmosphere.

Cassini was the first spacecraft to enter orbit around Saturn, and was by far the most sophisticated spacecraft to ever study the Ringed Planet, surpassing even the great Voyager I and II spacecraft which flew-by Saturn in 1980 and 1981. The Cassini spacecraft was outfitted with 12 major science instruments including visible, infrared, and ultraviolet imaging cameras, electric and magnetic field sensing antennas, in-situ ion and dust detecting instruments, a synthetic aperture radar, and radio science instrumentation. Cassini's science mission at Saturn included major investigations of the planet itself, its rings, Saturn's magnetosphere, the smaller icy moons of Saturn, and special emphasis was placed on the study of Saturn's largest moon, Titan.¹ To perform such wide-reaching scientific investigations, it was necessary for the Cassini spacecraft to fly a complicated orbital trajectory around Saturn that included 127 close gravity-assist flybys of Titan, which continually changed the size and orientation of Cassini's orbit around Saturn, thus enabling the spacecraft to study the Saturnian system from various orbital inclinations and distances. Flying the spacecraft along such an intricate orbital tour of the Saturnian system required continual orbit maintenance.

Specifically, the Navigation strategy for the Cassini mission consisted of using a series of three maneuvers between each pair of successive targeted flybys: a clean-up maneuver (~3 days after the previous flyby), a targeting maneuver (near apoapsis), and an approach maneuver (~3 days prior to the next flyby). Of those three, it was generally the targeting maneuver which was largest in size and accomplished the greatest deterministic orbit change, and these maneuvers most often occurred near apoapsis in Cassini's orbit around Saturn. The clean-up maneuver, which generally occurred ~3 days after the prior targeted flyby would serve the dual purpose of correcting trajectory position and velocity errors resulting from the small delivery errors during the previous flyby as well as to accomplish some of the deterministic ΔV to target the next flyby. The third and final maneuver in the series, the approach maneuver, generally occurred ~3 days before the next flyby of Titan and was always a purely statistical maneuver that was planned for the sole purpose of correcting any navigation error as late as possible before the next target flyby. This Navigation strategy, while requiring a substantial amount of ground support from both the Spacecraft Operations (SCO) and Navigation (NAV) teams, was used to extraordinary success for Cassini and achieved every single targeted flyby that was planned on the trajectory for the Prime Mission, Equinox Extended Mission (XM)³, and Solstice Extended-Extended Mission (XXM).⁴ Put simply, Cassini's trajectory was a masterpiece of interplanetary Mission Design and Navigation. There has never been any spacecraft that flew a trajectory with as many close targeted flybys used to achieve a gravity-assist and there has never been another spacecraft built by the Jet Propulsion Laboratory (JPL) with such demanding requirements on maneuver execution accuracy and total achieved ΔV .

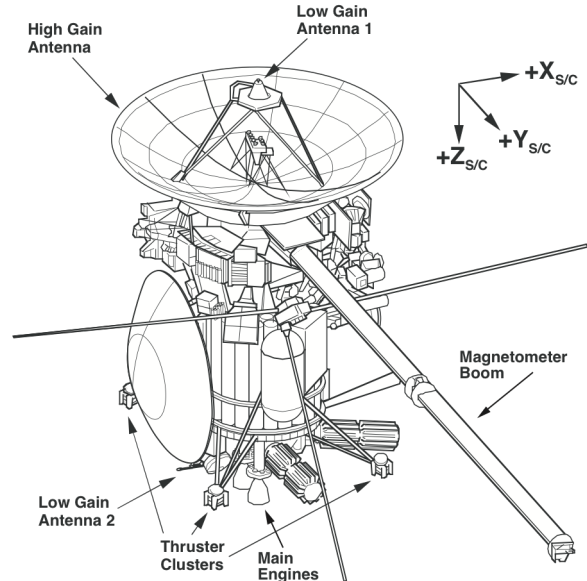


Figure 1. Cassini spacecraft mechanical configuration. This figure provides a depiction of the location of the RCS thruster clusters as well as the Main Engines and High Gain Antenna on the Cassini spacecraft.

This paper will focus on the performance of the Attitude and Articulation Control Subsystem (AACS) during these executed orbit trim maneuvers. Burk⁵ previously provided a similar summary of the Cassini AACS performance during ΔV maneuvers in 2005, but at that point the spacecraft had executed just 39 maneuvers (~10% of the ultimate total). This paper provides information for every maneuver executed between launch in 1997 and the final plunge in 2017. The Cassini spacecraft was required to perform maneuvers that met execution error requirements limiting both the magnitude error and pointing error of the maneuver. The excellent repeatability of the Cassini spacecraft during orbit trim maneuvers (OTMs) provides a clear demonstration of the achieved execution error across a wide range of spacecraft maneuver magnitudes. Indeed, the fact that Cassini executed every single one of its 360 maneuvers without ever terminating the burn prematurely or in error is testament to the highly reliable system that was engineered.

II. Spacecraft Attitude Control Hardware Overview

A depiction of the Cassini spacecraft mechanical configuration is shown in Figure 1. Cassini was a three-axis stabilized spacecraft that could use either reaction wheels or thrusters to maintain attitude control.^{6,7} Attitude determination was accomplished by using data from one of two redundant Stellar Reference Units (SRUs) coupled with high rate data from one of two redundant Inertial Reference Units (IRU). The Cassini spacecraft was equipped with sixteen 1 N reaction control system (RCS) thrusters, half in the prime set of thrusters (A-branch) and the other half in the backup thruster branch (B-branch). The RCS thrusters in each branch consist of four Y-facing thrusters which fired in opposing couples to provide torque around the spacecraft Z-axis (Figure 2) without any significant resultant ΔV , and four Z-facing thrusters which fired in uncoupled pairs to provide control authority around the spacecraft X-axis and Y-axis. The direction of the RCS thruster force vectors is shown pictorially in Figure 2. For attitude control, the RCS thrusters were used in either a traditional bang-bang control scheme, or an adaptive pulse width mode that further limited the total number of thruster cycles.⁶ However, it was also possible to use the RCS thrusters for small Orbit Trim Maneuvers (OTMs).⁸ For these small (<300 mm/s) maneuvers the RCS controller transitioned to an RCS ΔV mode where all four Z-facing thrusters fired simultaneously and X and Y axis attitude control was accomplished by briefly off-pulsing various pairs of the Z-facing thrusters.

In addition to the RCS thrusters, the Cassini spacecraft was also equipped with two 450 N bipropellant main engines, Main Engine A (ME-A) and Main Engine B (ME-B), which were affixed to the bottom of the spacecraft with two-axis gimbals that allowed the engines to control X and Y axis attitude errors when they were firing.^{5,7,8} Z-axis control during Main Engine maneuvers was still performed using the coupled Y-facing RCS thrusters. Main Engine A (ME-A) was the only main engine used by Cassini during its 20-year mission. The actuators for ME-B were regularly exercised for hardware maintenance, but the backup main engine was never fired at any point in the mission. The Cassini main engine was used for all maneuvers greater than approximately 300 mm/s.

The large number of executed Cassini maneuvers provided the operations team with a rich dataset of flight telemetry for spacecraft attitude dynamics during maneuvers. With the Cassini flight data, the AACS team was able to observe long term gradual changes in RCS duty cycle behavior, center of mass offset changes, and attitude control error, among other changes. These Cassini maneuvers occurred across a wide range of spacecraft mass properties.

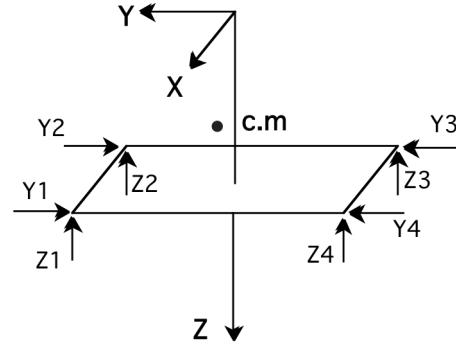


Figure 2. Cassini RCS thruster pointing. *The relative pointing directions of the eight RCS thrusters used for attitude control and ΔV maneuvers are depicted relative to the body fixed Cartesian coordinate system. The A-branch thrusters and their B-branch counterparts are identically oriented and nearly co-located.*

III. Cassini Maneuver Statistics

The Cassini Mission Design and Navigation (NAV) teams planned a total of 502 maneuvers over the course of the 20-year mission. Of those planned maneuvers, the Spacecraft Operations Team (SCO) ultimately executed 360 maneuvers (the remaining 142 were cancelled or never fully planned). A full list of the pertinent information for every executed Cassini maneuver is included in the Appendix (Section X), and a timeline of when those maneuvers occurred is shown in Figure 3. The first maneuver executed by Cassini was TCM-001, which occurred just 25 days after launch (1997-313). The final maneuver of the mission was OTM-472 (on 2017-196), which occurred 62 days before Cassini was intentionally crashed into Saturn to dispose of the spacecraft.

For the Cassini mission, maneuvers that occurred between launch and Saturn Orbit Insertion (SOI) were called Trajectory Correction Maneuvers (TCMs) and maneuvers after SOI were called Orbit Trim Maneuvers (OTMs). With this maneuver naming convention, it was always easy to determine whether a maneuver occurred prior to Saturn arrival (TCMs) or following Saturn arrival (OTMs). In addition, every OTM during the Saturn science tour was planned to have a prime maneuver window and a backup maneuver window, that typically fell ~24 hours after the prime window. The backup maneuver window was included in the plan primarily to protect against ground issues with the Deep Space Network (DSN) that might interfere with the ability to uplink a maneuver sequence to the spacecraft, though it also protected against a subset of spacecraft anomalies. To avoid the need to rush the development of the backup maneuver in the event that the primary maneuver uplink failed, the NAV and SCO teams typically designed both the prime and backup maneuver sequences in parallel. The prime maneuver was given the label “OTM” and the backup maneuver was given the label “JTM.” What the letter “J” originally stood for has been lost to posterity. The quality of support from the Deep Space Network over Cassini’s 20-year mission was outstanding, and meant that a JTM (backup) maneuver was only once required due to ground support/uplink issues. However, there were a handful of instances during the mission where there were navigation or operational reasons why it was preferable to execute the backup (JTM) maneuver instead of the prime maneuver (e.g. to save a small amount of fuel, or to avoid impacting spacecraft science pointing during important observations).

The maneuver *numbering* that was used by the Cassini mission was sequential but with non-intuitive exceptions. Some maneuver integers were skipped and other integers were repeated with single letter suffixes. For example, Cassini executed TCM’s named TCM-019, TCM-019a, and TCM-019b, as well as OTM-010a, OTM-164a, and OTM-183x. The Navigation team had a method to their numbering too convoluted to detail here, but suffice it to say that not every OTM number was used in their planning and some numbers were reused. However, thankfully, it is true that OTM and JTM numbers grew monotonically over the mission (e.g. OTM-183 was before OTM-183x, which was itself before OTM-186).

In Figure 3, the reader will note that the pace of maneuver execution was substantially lower during the interplanetary cruise (1997-2004) and then picked up to a roughly constant rate during the Saturn tour (2004-2017). As previously mentioned, Cassini could execute ΔV maneuvers using either its bipropellant 450 N Main Engine (ME-A) for maneuvers greater than approximately 300 mm/s, or with its monopropellant 1 N RCS attitude control thrusters

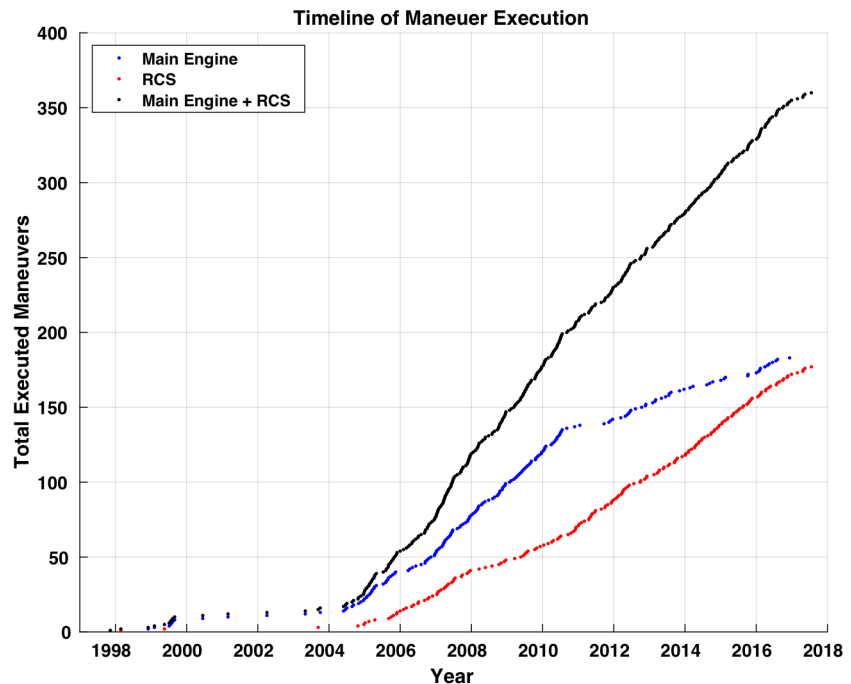


Figure 3. Timeline of maneuver occurrence. The running total of Main Engine maneuvers, RCS maneuvers, and the sum of both is shown over time from launch in 1997 to the end of the mission in 2017. Note that maneuvers were relatively infrequent during the interplanetary cruise (1997-2004) and Main Engine maneuvers became less frequent during the XXM.

for maneuvers less than 300 mm/s, and Figure 3 shows the relative number of ME versus RCS maneuvers that were executed. The total number of ME maneuvers executed during the Cassini mission was 183 and the total number of RCS maneuvers executed was 177. It is a coincidence that the total number of ME and RCS maneuvers is as close as it is. During the Prime Mission and Equinox Extended Mission (XM), larger ΔV maneuvers were included to complete Cassini's ambitious mission objectives within the relatively short 4-year prime mission duration and 2-year extended mission duration. When it came time for JPL's Mission Designers to design the Solstice Mission (XXM) trajectory³, the remaining spacecraft propellant was quite limited and so the total deterministic ΔV included in that trajectory was lower and the average maneuver size was smaller. As a result, the frequency of Main Engine maneuvers was larger during the Prime Mission (2004-2008) and the XM (2008-2010) than it was during the XXM (2010-2017). The frequency of RCS maneuvers remained approximately constant during the entirety of the Saturn Tour.

To give a sense of the cadence of maneuver execution, consider Figure 4, which shows the time between successive executed Cassini maneuvers. The gap between maneuvers during the interplanetary cruise (1997-2004) could be as long as a full year, but after Cassini arrived at Saturn, the pace of maneuver execution increased. The histogram in Figure 4 shows that during the Saturn Tour phase of the mission, the most common interval between successive maneuvers was 4-7 days. A total of 130 of the 360 executed maneuvers fell less than 1 week after the previously executed maneuver, and 285 (80%) occurred less than 3 weeks after the previous maneuver. The shortest turnaround between successive maneuvers

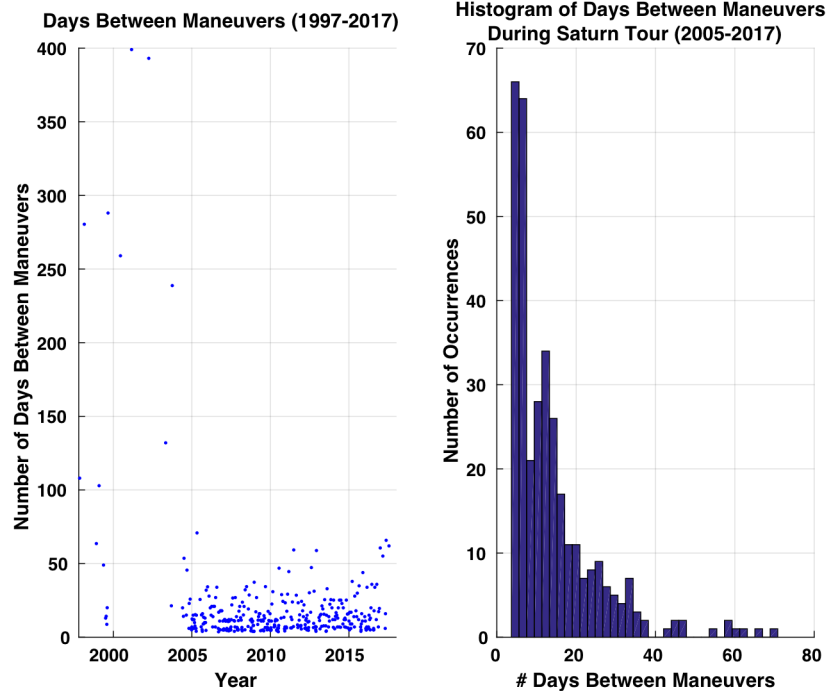


Figure 4. Elapsed time between executed Cassini maneuvers. *The left-hand plot shows the number of days between consecutive executed maneuvers from 1997 to 2017. The right-hand plot shows a histogram of the data on the left and shows the relative frequency of different gap durations between maneuvers.*

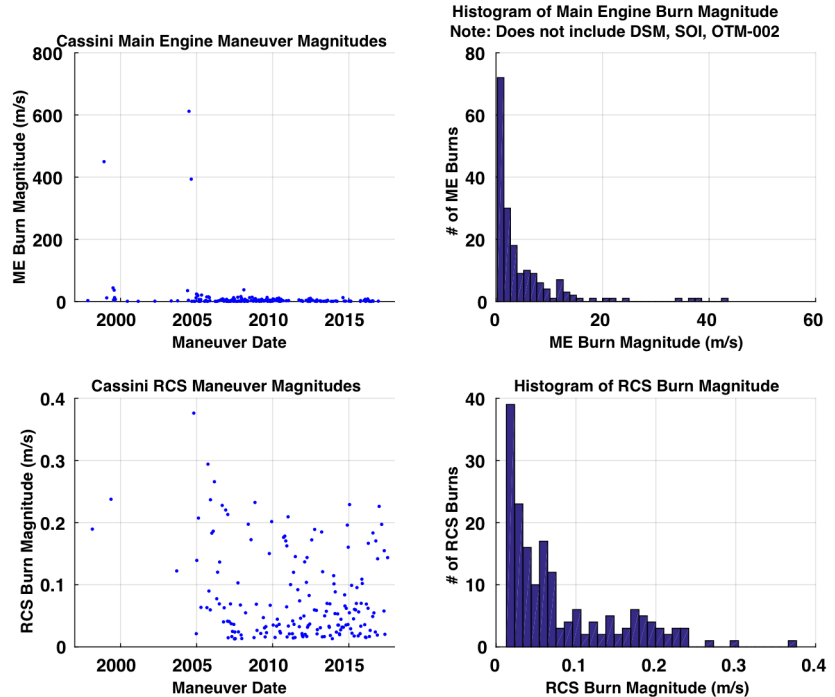


Figure 5. Main Engine and RCS maneuver magnitudes. *The magnitudes of all ME maneuvers are at the top shown as a function of time (left) and as a histogram of number of occurrences (right). The RCS maneuver magnitudes and the corresponding histogram are shown in the bottom two plots. The three largest maneuvers were SOI, TCM-005, and OTM-002.*

during the Cassini mission was the 3 days 16 hour gap between OTM-071 (2006-253) and OTM-072 (2006-257), and the longest gap was the 399 days from TCM-017 (2001-059) to TCM-018 (2002-093). During the Saturn Tour (2004-2017) it was relatively uncommon for more than 1 month to transpire without a maneuver. The 22 Proximal Orbits during the final phase of Cassini's mission were originally designed to be ballistic (i.e. no maneuvers required), so it is not surprising that the two longest gaps between maneuvers during the Saturn Tour were the 65-day gap between the final two maneuvers (OTM-471 on 2017-130 and OTM-472 on 2017-196) and the 62-day gap between OTM-472 and the Saturn impact on 2017-258.

A time history and histogram of the magnitude of the executed Cassini maneuvers is shown in Figure 5 and, for clarity, the Main Engine maneuvers are separated from the RCS maneuvers. The largest maneuver executed over the course of the 20-year mission was the Saturn Orbit Insertion (SOI) burn in 2004 at 626.17 m/s, and the smallest maneuver executed was OTM-364 in 2013 at 8.3 mm/s, so maneuver sizes varied across a full 5 orders of magnitude. The histograms in Figure 5 show that 68% of the Main Engine maneuvers were less than 5 m/s, with the remaining 32% ranging from 5 to 600 m/s. Among the RCS maneuvers, 66% of these maneuvers were below 80 mm/s with the remaining third spanning from 80 to 376 mm/s. It is evident in the top left pane of Figure 5 that there are three large outlier maneuvers among the Main Engine maneuvers. Those three maneuvers are the 449.7 m/s Deep Space Maneuver (DSM, also called TCM-005), the 626.17 m/s Saturn Orbit Insertion (SOI) burn, and the 393.4 m/s Periapsis Raise Maneuver (PRM, also called OTM-002). Those three maneuvers alone consumed 69% of the 3000 kg of bi-propellant that Cassini launched with, with the remaining 180 executed main engine maneuvers drawing from the remaining ~31%.⁵ In fact, of the 5573 kg that the spacecraft weighed at launch, 56% of that mass (3132 kg) was either bi-propellant fuel (MMH), oxidizer (N2O4), or hydrazine monopropellant for the RCS thrusters.

On the topic of the spacecraft mass, the time history of the spacecraft mass and remaining propellant are shown in greater detail in Figure 6. In Figure 6 the spacecraft wet mass (spacecraft structure + liquid propellants) is shown in blue relative to the estimated spacecraft dry mass (dotted black line). In addition, the three liquid propellant types are also shown individually. Note that the step-decrease in the spacecraft dry mass in late 2004 corresponds to the release of the 320 kg Huygens Probe, which was released by Cassini on Christmas Day 2004 and landed on Titan in January 2005.² Since the majority of the spacecraft mass properties changes occur prior to 2005, the right-hand plot zooms-in to provide more detail of the remaining propellant during the last 12 years of the mission. At the time Cassini crashed into Saturn, it is estimated that 59 kg of bipropellant of the original 3000 kg load remained. This would correspond to ~2% of the launch load. The Cassini Prop team could estimate the remaining propellant using a combination of engine valve on-time and propellant tank pressure transducers, but the accuracy of their estimate at the end of the mission was only within +/- a few percent. As a result, there was a very real concern during the final few Main Engine maneuvers that the bipropellant would be exhausted, and contingency plans were prepared to execute cleanup maneuvers (if needed) with the monoprop RCS thrusters in the event that the bipropellant ran out in the middle of an ME maneuver. At the end of the Cassini mission, ~34 kg of hydrazine monopropellant, from the original 132 kg launch load (25%) remained. If it had been possible to avoid the planned impact with Saturn that occurred at the end of the Proximal Orbit ballistic trajectory, the 34 kg of remaining hydrazine would have been enough for several additional years of science operations. So, to summarize, Cassini ended its mission with the bipropellant virtually exhausted, but with ample hydrazine monopropellant to execute all planned science observations while maintaining substantial margins for unplanned usage.

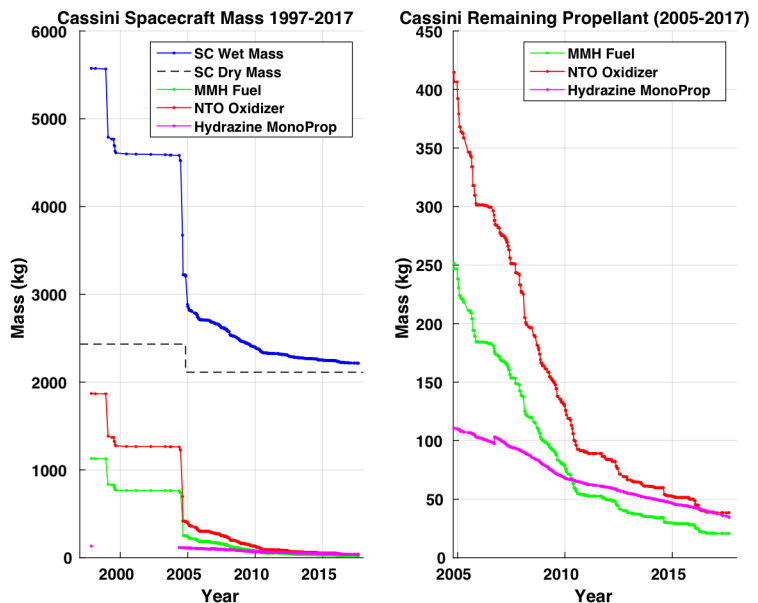


Figure 6. Cassini total spacecraft mass and remaining propellant mass. The left-hand plot shows the total SC mass (blue) slowly being depleted by ΔV maneuvers and the deployment of the Huygens probe. The right-hand plot focuses in on the remaining bipropellant (red and green) and monopropellant (magenta) masses during the final 12 years of the mission. The small increase in the monopropellant mass resulted from a modeling update that the Prop team made following a one-time helium pressure recharge.

IV. Maneuver Sequence Overview

Even before launch, the team planning for the Cassini mission knew that the large number of maneuvers and the relative frequency of the maneuvers would present a challenge to the operations team. Human error is always a risk when a complex operations activity is repeated frequently, even more so when the task is repeated hundreds of times spread across two decades and with many successive generations of new replacement engineers being added to the operations team. To ensure that error-free maneuver sequences could be designed in a fixed amount of time, the Cassini project developed ground software that could be used to design maneuvers of any size and in any direction following a strictly parameterized maneuver sequence template. In operations, the AACS, Systems, Propulsion, and Navigation teams had maneuver planning and design procedures that were followed by all team members to provide consistency of output. Those procedures were living documents that were iteratively updated in response to issues that naturally arose over the years.

The maneuver sequence unfolded as follows: For each maneuver the spacecraft would always start at an attitude that had the High Gain Antenna (HGA) either pointed at the Sun (during the inner solar system cruise) or at the Earth during the Saturn Tour (2005-2017). The maneuver ΔV direction (provided by the NAV team) was a fixed vector defined relative to the inertial J2000 coordinate frame. For each maneuver, the spacecraft would first perform a “roll” slew around the SC $-Z$ axis (the HGA pointing axis) to reorient the spacecraft such that after the slew the inertial ΔV vector was located in the spacecraft YZ plane.⁵ The roll slew could be any angle between -180 to $+180$ degrees around the $-Z$ -axis. Next, a second “yaw” slew of 0 to -180 degrees around the SC $+Y$ axis was performed to align the SC Z -axis with the desired burn direction. The maneuver was then performed by firing the ME engine or RCS thrusters until the commanded burn magnitude was achieved. After the maneuver cutoff and some settling time, the spacecraft then performed “unwind yaw” and “unwind roll” slews which were the reverse of the slews used to get to the ΔV attitude, and these unwind slews returned the spacecraft to its starting attitude.

It should be noted that Cassini had the ability to perform Euler-Axis/Euler-Angle slews, so it was possible to reorient the spacecraft from any starting attitude to any ending attitude with a single slew. So, it would have been possible to slew to and from the burn attitude with a single slew, but this was never done due to thermal constraints and to avoid placing the sun inside keep-out cones of the SRUs and sensitive science instruments.^{5,7}

During the interplanetary cruise, Cassini ventured into the inner solar system to achieve two gravity-assist flybys of Venus. These Venus flybys placed the spacecraft for several months in a very harsh thermal environment due to the sunlight intensity. The harsh solar irradiance environment required that the spacecraft remain at an attitude where the 4-meter diameter High Gain Antenna (HGA) was pointed at the sun so that the majority of the spacecraft was hidden in the shadow of the HGA. However, this “sun shield” strategy could not be used during trajectory correction maneuvers, and so there was an allowance that the spacecraft could spend short periods (less than 2 hours) at attitudes where the HGA was not pointed at the sun.⁵ It was this thermal constraint that primarily drove the use of the two-turn “roll” and “yaw” strategy to get to the burn attitude. The “roll” slew around Z kept the spacecraft shaded by the HGA and the Y “yaw” slew minimized the amount of time that the spacecraft left the “sun shade” attitude, and always slewed in a direction that kept the thermally-sensitive $+X$ hemisphere of Cassini at least 90° away from the Sun.

After the spacecraft had arrived at Saturn, the thermal constraint was no longer applicable, but Cassini continued to use the two turn roll and yaw strategy to get to the maneuver attitude because these slews guaranteed that: (1) the Sun would never be in the SRU field of view, (2) the sun would never shine on the sensitive science instrument radiators that were on the $+X$ side of the spacecraft, (3) the sun would never shine into the sensitive science camera optics that were pointed in the $-Y$ direction, and (4) the roll/yaw strategy also kept the HGA pointed at Earth for the maximum amount of time possible during the maneuver.⁵ Keeping the HGA pointed at Earth meant that real-time monitoring of the maneuver sequence was possible until the spacecraft performed the yaw slew away from the Earth-line.

During the inner solar system cruise the spacecraft had not yet begun using RWA control and so the slews to and from the burn attitude were performed using RCS thruster control. Once the spacecraft-sun distance grew sufficiently large, the spacecraft transitioned to RWA control and the maneuver sequence began to incorporate slews under RWA control. For RCS OTMs both the roll and yaw slews were performed on RWA control. Although the RWA-controlled slews were slower due to the smaller control authority of the wheels, the use of RWA control was desirable for maneuvers because the RCS thrusters did not impart any incidental ΔV during the slews to/from the burn attitude. Recall that the Z -facing RCS thrusters, which are used for X and Y axis control, fire in uncoupled pairs that impart ΔV . For RCS maneuvers, after RWA control was used to slew to the maneuver attitude, the spacecraft transitioned to RCS control just before the maneuver began and the RWAs were put into a spin-rate control mode, so they held a constant spin-rate but were no longer controlling attitude. After the maneuver completed and a settling time had

elapsed, the spacecraft transitioned back from RCS to RWA control and the spacecraft then slewed back to the starting downlink attitude.

For Main Engine maneuvers, it was not possible to leave the RWAs on and spinning during the maneuvers. Cassini's radioisotope thermoelectric generators (RTGs) did not produce enough power to drive the three prime reaction wheels while also driving the bipropellant latch valves and the Main Engine gimbal actuators. Thus, for Main Engine OTMs during the Saturn Tour, the spacecraft still performed the first "roll" slew on RWA control, but then Cassini would transition to RCS control and the RWAs were fully spun-down and powered off and the "yaw" slew to the burn attitude was then performed using RCS control. It was desirable to spin-down the RWAs while the HGA was still Earth-pointed so that there was radiometric Doppler data for the Navigation team to estimate the resultant ΔV from the wheel spin-down, and additionally, if the RWA spin-down (and spin-up after the maneuver) had been performed after the yaw slew completed, then the total time that the spacecraft HGA was pointed away from Earth would have been extended by ~1-1.5 hours.

Cassini carried a single-axis accelerometer aligned with the SC Z-axis.^{5,7} The data from the accelerometer was integrated during Main Engine maneuvers to determine when the commanded ΔV had been accumulated and cutoff should occur. The accelerometer was generally powered off during the mission, but it was powered on 1 hour before each Main Engine maneuver so that it was allowed to reach a steady-state operating temperature before its data was used. After the roll/yaw slews to the burn attitude had completed, the accelerometer bias was calibrated for 1 minute (this occurred just 3 minutes before the burn ignition). The accelerometer was not used for the cutoff of the RCS maneuvers because the relatively weak 1 N RCS thrusters produced insufficient force to be reliably measured by the accelerometer. Instead, for RCS maneuvers the spacecraft was provided with estimates of the RCS thrust and spacecraft mass properties in order to model the acceleration time history and the maneuver was cutoff after sufficient RCS on-time had accumulated. In effect, this was a more sophisticated way of performing a "timed burn".

For main engine maneuvers, many other events occurred as part of the maneuver sequence in order to prepare for the firing of the main engine. These events included software changes to set the desired telemetry channels and sampling frequencies, and hardware changes including powering on both the bipropellant latch valve drive electronics, and the main engine valve drive electronics and opening the latch valve upstream of the main engine. In addition, maneuver sequence also powered on the engine gimbal electronics and "stroked" the Main Engine gimbals from side-to-side so that the gimbal seals were broken free from the position that had been static at for many days or weeks. At the end of the stroking, the engine gimbal was positioned to its "preaim" position in preparation for burn ignition. For Main Engine maneuvers, following burn ignition the engine remained burning continuously at a 100% operating duty cycle. The engine gimbals reoriented the ME pointing direction to control X and Y attitude error and keep the main engine pointing in the direction of the desired inertial ΔV direction.

V. Maneuver Duty Cycle

Unlike the Main Engine maneuvers, where the engine was operated at 100% duty cycle, for the RCS maneuvers the thrusters were off-pulsed resulting in a lower average duty cycle. RCS maneuvers did begin with all four Z thrusters fully on. However, the thrusters needed to be off-pulsed during the RCS maneuvers because the effective force vector from the four firing Z-facing thrusters was aligned with the Z-axis (apart from small thruster-to-thruster variations in force magnitude and slight mechanical misalignments), but the SC center of mass did not lie on the SC Z-axis. The CM offset from the Z-axis resulted in the effective lever-arm of the four Z-facing thrusters varying from thruster to thruster. The different lever-arms between the four Z thrusters produced torques around the SC X and Y axes that resulted in attitude and rate errors, and so the thrusters were off-pulsed to correct the X and Y attitude and rate error.

Over the course of the mission, the AACCS team began monitoring the reconstructed duty cycle telemetry from each RCS maneuver with increasing interest and vigilance. Ultimately, the duty cycle telemetry from the RCS maneuvers became one of the most important methods by which the SCO team could monitor the health of the various thrusters. To illustrate this point, consider the plots of the average duty cycles for all RCS maneuvers that are plotted in Figure 7. Each colored line in Figure 7 shows the time history of the average RCS duty cycle over the course of one RCS maneuver. The duty cycle is defined as the total on-time of the RCS thrusters divided by the total time that has elapsed since the start of the burn. The duty cycles for each of the four Z-facing thrusters could also be individually computed, but for simplicity we'll restrict our current discussion to the average across the four RCS thrusters. As a reminder, Cassini was launched with both a prime set of eight RCS thrusters (called the A-branch) and a backup/redundant set of eight RCS thrusters (called the B-branch). The prime and backup thrusters were co-aligned, and very nearly co-located, so that the difference in lever arm between prime and backup branches was relatively small. From the time that Cassini launched (1997) until early 2009, Cassini used exclusively the A-branch of RCS

thrusters for both attitude control and RCS maneuvers. The average duty cycle for the RCS maneuvers executed on the A-branch of thrusters is shown in the upper plot of Figure 7. The color-mapping for Figure 7 shows the evolution of the duty cycle average over time (cooler shades being older data and warmer shades being more recent). Two black arrows in the upper plot of Figure 7 direct attention to the two final long RCS maneuvers that were performed on the A-branch, and note that early in these maneuvers the two lines dropped to lower average duty cycle values than the RCS maneuvers that had occurred shortly before those maneuvers. This was an early indication of a thruster anomaly.⁹

As backstory, in late 2008, Cassini executed two relatively long RCS maneuvers where the total RCS on-time matched closely with the ground predict, but the achieved ΔV that was measured by the Navigation team's radiometric Doppler data showed anomalously low underperformance (i.e. achieved less ΔV than desired).¹⁰ It was concluded from "rough" chamber pressure telemetry in two of the A-branch Z-facing thrusters that Cassini was experiencing anomalous thrust degradation in two of its Z-facing thrusters.⁹ Various causes for the degradation were proposed.⁹ Regardless of the cause, the Project Manager agreed with the recommendation of the Prop, NAV, and AACs teams that the spacecraft should swap to the backup B-branch of thrusters.¹⁰ Prior to the thruster branch swap, a total of 48 RCS maneuvers had been performed using the A-branch thrusters. The thruster swap occurred in early 2009¹⁰, and all subsequent RCS controlled activities and RCS maneuvers (from 2009-2017) were executed with the B-branch thrusters. A total of 129 RCS maneuvers were executed on the B-branch, so the AACs team ended up with 2.5x more data on RCS maneuver performance from the B-branch.

The average RCS duty cycle time history for the RCS maneuvers performed with the B-branch thrusters is shown in the lower half of Figure 7. Whereas the average duty cycle of the A-branch thrusters had changed abruptly multiple times due to the large variations in SC mass properties between 1997 and 2008, no large SC mass properties changed occurred after 2005 (e.g. Huygens probe release), and so the B-branch duty cycle data evolution shows a very predictable trend. As the spacecraft slowly expelled the remaining bipropellant and monopropellant, and as the total

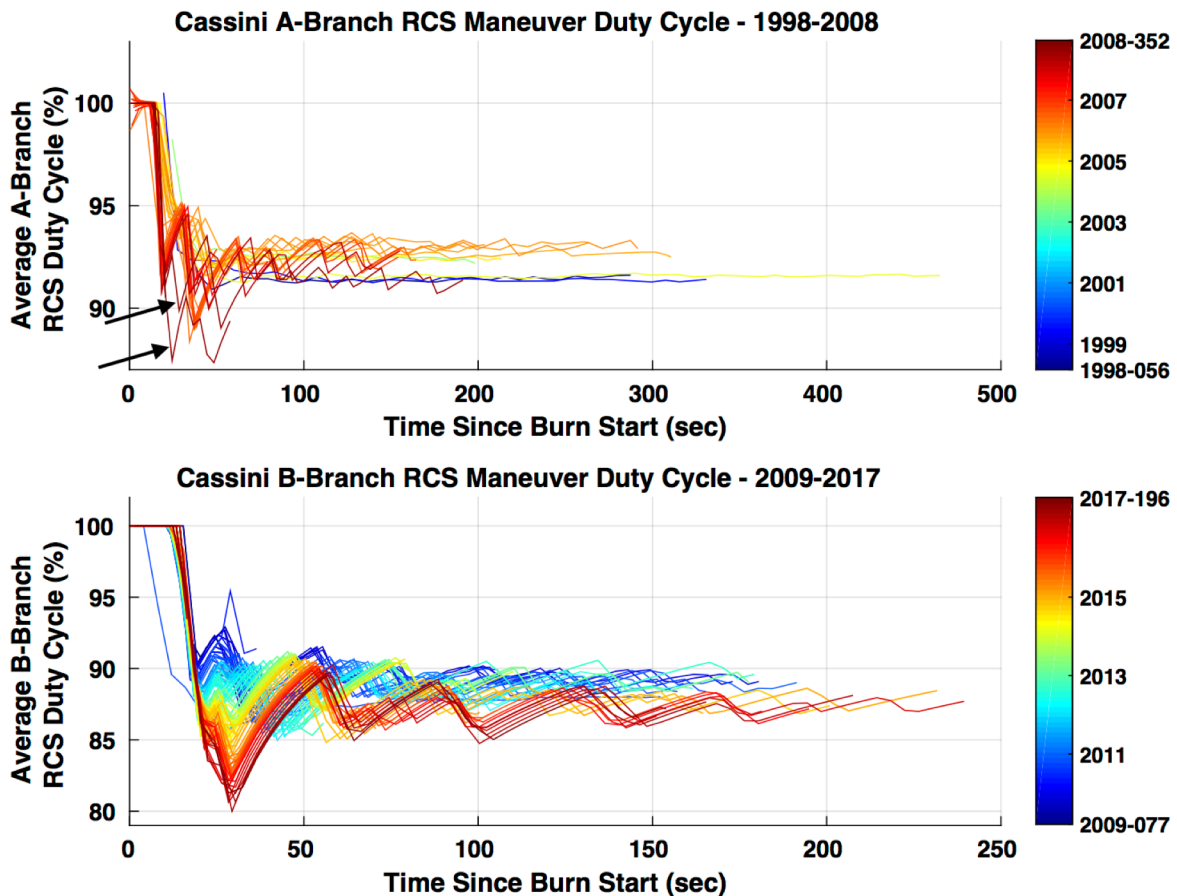


Figure 7. Cassini average A-branch and B-branch RCS maneuver duty cycles. *The average duty cycle (accumulated on-time divided by total time since burn ignition) of the four z-facing RCS thrusters is shown as a function of time during the maneuvers for the A-branch RCS maneuvers on top and B-branch maneuvers on the bottom. The color-mapping is used to show the passage of time, with cooler shades corresponding to older maneuvers and warmer shades to more recent maneuvers*

thrust of the blowdown RCS monoprop thrusters decayed, the average effective RCS duty cycle continued to decrease to lower and lower values. The gradual decrease in duty cycle was driven primarily by the changing spacecraft mass properties. As the spacecraft expelled propellant, the center of mass shifted in a direction that resulted in a larger thruster effective lever-arm mismatch, and therefore more off pulsing (i.e. lower duty cycles) for the thruster with the longer lever arm was required.

This decreasing duty cycle trend is especially evident in the spread of the curves in the range of 20-50 seconds into the maneuver, but it also apparent in the final values (extreme right end) of each of the lines. From 2009-2017 the Prop and AACS teams watched the average duty cycle trend plot closely to try to spot abrupt changes in duty cycle behavior, which might be the first indications of anomalous B-branch thruster degradation. However, as the lower plot in Figure 7 shows, the duty cycle evolution from 2009-2017 continued in such a smooth and predictable manner, that the SCO team ultimately concluded that no hardware degradation was evident in the B-branch even after 8 years of use. Although the progressively lower duty cycles in the B-branch data of Figure 7 may at first seem to be undesirable, counterintuitively the opposite was actually true. As will be shown later, the lower average RCS duty cycles corresponded to SC attitude errors that more closely approached the desired maneuver pointing direction, and thereby decreased the maneuver pointing error.

VI. Main Engine Gimbal Pointing Changes During Mission

The Cassini Main Engines (ME-A and ME-B) were mounted on the +Z end of the spacecraft, but they had a translational offset of ~ 24 cm from the spacecraft Z-axis in the Y direction (+Y for ME-A and -Y for ME-B).⁵ To counter the offset from the mechanical centerline, the Main Engine nozzles were canted 7 degrees from the SC +Z axis. During each Main Engine maneuver the misalignment between the ME thrust vector and the spacecraft center of mass (CM) could have easily caused the spacecraft to tumble, and so it was necessary for each of the main engines to have a two-axis gimbal platform so that spacecraft X and Y axis attitude could be controlled during the maneuver. The ground operations team kept running estimates of the current location of the spacecraft CM in the spacecraft body frame.⁵ Prior to each maneuver the engine gimbals were commanded to point ME-A in the direction of the estimated spacecraft CM. This would minimize the amplitude of the attitude transients that occurred immediately following burn ignition.

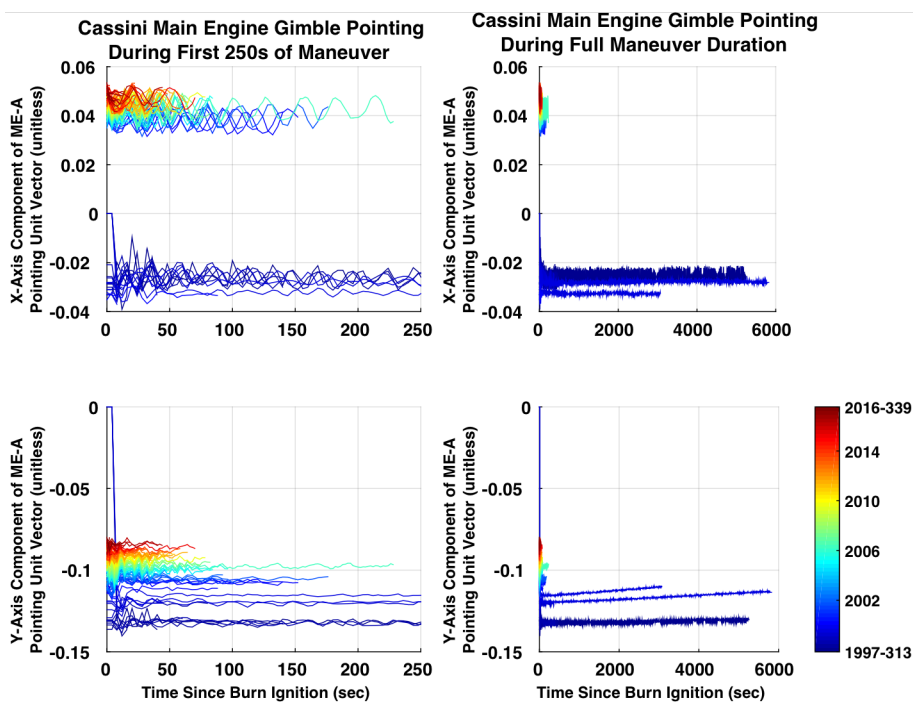


Figure 8. X and Y axis components of Main Engine gimbal pointing during maneuvers. The X & Y components of the ME pointing unit vector in the SC body frame are shown for all ME maneuvers of the mission. The left-hand plots show the gimbal pointing for the first 250 seconds of the maneuver and the right-hand plots zoom out to show the behavior across even the longest maneuvers. Note the gradual trends to higher values on the left as the mission progressed and during the course of the longest 3 maneuvers on the right due to propellant depletion altering the spacecraft CM location.

After burn ignition, the ΔV attitude controller logic commanded the ME gimbal to move as necessary to actively minimize X and Y axis pointing errors. The pointing of the Main Engine during a maneuver can be pictured as a time varying unit vector in the spacecraft body frame. The vast majority of that vector will be in the SC -Z direction with small deflections in the +/-X direction being used to control Y-axis attitude error and, similarly, small deflections in the +/-Y direction being used to control X-axis attitude error. The time history of the X and Y axis components of the ME-A pointing unit vector is shown for all Main Engine maneuvers in Figure 8. In

this figure, the color-mapping is used to show the passage of time, with the cooler shades corresponding to maneuvers early in the mission and the warmer shades corresponding to the most recently occurring maneuvers. An examination of the X-axis component of the ME pointing (upper plot) had a negative polarity prior to the Huygens probe release in 2004 and then switched to a positive polarity after Huygens was released. This makes sense, since the 320 kg Huygens probe was mounted on the $-X$ side of the spacecraft and offset from the center line of the spacecraft. Once the probe was released, the total system center of mass shifted from the $-X$ side of the YZ plane to the $+X$ side. In the bottom-left plot of Figure 8 there is a clear trend where the Y-axis component of the ME pointing vector moved gradually in the $+Y$ direction (towards zero) over the course of the mission. This was also the result of the changing spacecraft mass properties over the course of the mission. Although the polarity of the X-axis component swapped from negative (before the Huygens probe release) to positive (after the probe release), the Y-axis pointing component remained negative for the entire mission due to the fact that mounting location of ME-A was translated 24 cm from the Z-axis toward $+Y$. Although ME-B (the backup main engine) was never used, the expectation is that the Y-axis component of the ME-B to CM vector would have had a $+Y$ component that was roughly a mirror image of the data from the use of ME-A.

Note that the left-hand plots in Figure 8 cut off after 250 seconds (4.2 minutes) so that detail of the many short ME maneuvers is visible, but the right-hand plots extend for the full duration of the longest ME maneuvers. The longest three were Saturn Orbit Insertion (97 min), the Deep Space Maneuver/TCM-005 (88 min), and the Periapsis Raise Maneuver/OTM-002 (51 min). It is interesting to note that for the three longest maneuvers of the mission, there is a linear change in the Y-axis component of the ME-A pointing over the course of the long maneuvers. This corresponds to the shifting location of the spacecraft center of mass as large quantities of propellant mass are expelled during those maneuvers.

One mystery that the AACS team has tracked for the full duration of the mission is an oscillation in the main engine pointing direction of ~ 25 -30 second period (0.03-0.04 Hz) that persists across even the longest ME maneuvers. Lee⁷ previously published a conjecture that the 30s oscillation was the result of non-linear actuator motion, such as gear backlash. There were no new insights about the 30s oscillations since 2005, so the description provided by Lee and Hanover⁷ at that time remains the preferred explanation of the Cassini AACS team. The oscillation was visible in longer ME maneuvers all the way to the end of the mission.

For all ME maneuvers, the initial pointing direction of the Main Engine was aligned with a “preaim” vector that was the ground-derived best estimate of the ME-A nozzle to SC center of mass vector based on telemetry from the most recent sizable main engine maneuver. The preaim vector direction was used to set the initial orientation of the

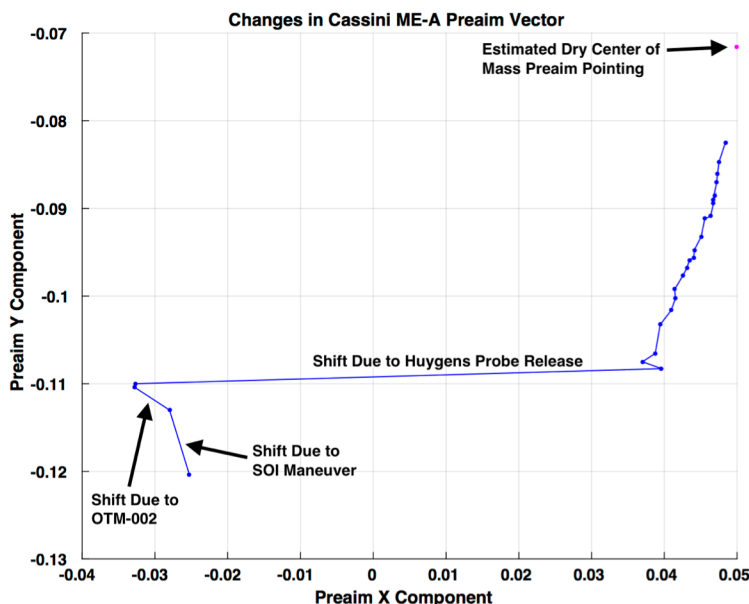


Figure 9. Cassini ME-A preaim vector X & Y components during the mission. *The preaim is the direction the ME-A engine was pointed prior to ignition to try to point through the CM location. Large changes in preaim pointing resulted from the expulsion of mass during the large maneuvers and from the Huygens probe deployment.*

gimbal prior to the maneuver, but after burn ignition, the gimbal was free to reorient the nozzle however necessary to maintain X and Y axis attitude control. In Figure 8, four of the earliest maneuvers begin with the X and Y components of the ME pointing being zero (i.e. the gimbal is parallel to the SC Z axis). This is a telemetry artifact indicating that the telemetry values were uninitialized at the start of the burn, but the engine was actually aligned with a ground derived “preaim” vector.

A history of changes of the on-ground estimate of the ME-A to CM (i.e. preaim) pointing vector that span from TCM-020 to the end of the mission is shown in Figure 9. In this figure, the X-axis preaim vector component is plotted against the Y-axis preaim vector component. Since the vast majority of the preaim vector is in the $-Z$ direction, this plot is akin to looking down the tip of the preaim vector so that the side-to-side (X and Y) deviations are easily visible. This plot doesn’t capture the preaim motion that resulted from the mass expelled during the DSM maneuver (TCM-005) but

does capture the remainder of the mission. Figure 9 shows that there were substantial changes in the preaim pointing direction following the large SOI and Periapsis Raise Maneuver (OTM-002) maneuvers, but by far the most dramatic change in the preaim pointing direction resulted from the release of the Huygens Probe. The stray magenta dot on the upper right corner of Figure 9 shows to the best estimate of where the preaim vector direction would be for the completely dry spacecraft mass properties. This would correspond to a case where Cassini had expelled all of the MMH and Nitrogen Tetroxide oxidizer bipropellant, all hydrazine monopropellant was expelled, and all helium pressurant for both the biprop and monoprop tanks was also expelled. Since Cassini ended its mission with tens of kilograms of each of those propellants still in the tanks, the magenta dot is purely hypothetical.

VII. Maneuver Execution Error

The key metric for the evaluation of the Cassini maneuver performance is the measured maneuver execution error.^{5,7,8} Cassini, like numerous other JPL missions, specifies requirements for maneuver execution accuracy based on an execution error model proposed by Gates.¹¹ In the Gates model, the maneuver execution error is the difference between the commanded burn vector, \bar{V}_C , and the achieved burn vector, \bar{V}_A . This execution error is broken into a magnitude error, $\bar{e}_{Magnitude}$, that is parallel to the commanded burn direction and a pointing error, $\bar{e}_{Pointing}$, that is perpendicular to the commanded burn direction. The magnitude and pointing error vectors can be computed as shown in Equation 1 and 2, where \bar{V}_C and \bar{V}_A are the commanded and achieved burn vectors, and \bar{v}_C and \bar{v}_A are the unit vectors parallel to \bar{V}_C and \bar{V}_A respectively.

$$\bar{e}_{Magnitude} = \bar{V}_C - (\bar{V}_A \cdot \bar{v}_C)\bar{v}_C \quad (1)$$

$$\bar{e}_{Pointing} = \bar{V}_A - (\bar{V}_A \cdot \bar{v}_C)\bar{v}_C \quad (2)$$

The allowable sizes of magnitude and pointing errors is parameterized in the Gates model with four Gaussian distributed error terms: a fixed magnitude error, a proportional magnitude error, a fixed pointing error, and a proportional pointing error.^{5,7,11} Thus, larger burns are allowed to have larger magnitude and pointing execution error ΔV , provided that the error only grows in proportion to the maneuver size. The *fixed* magnitude and pointing error terms are used in recognition of the fact that for very short maneuvers it is possible for error sources (e.g. startup and cutoff transients) to make up a significant fraction of the total ΔV . Without an allowance for fixed error terms, there would be a natural tendency for small maneuvers to appear to be less accurate, when in fact they are simply less repeatable due to the low “signal to noise” between the commanded ΔV and the error source ΔV .

For Cassini, the maneuver execution error requirements for the 1σ error bounds are shown in Table 1.

Table 1. Maneuver Execution Error Requirements for the Cassini Mission.

	Main Engine Maneuver		RCS Thruster Maneuver	
1σ Requirement	Proportional	Fixed	Proportional	Fixed
Magnitude Error	0.2%	10 mm/s	2.0%	3.5 mm/s
Pointing Error	3.5 mrad	17.5 mm/s	12.0 mrad	3.5 mm/s

The computed magnitude and pointing error terms (Eq. 1 and Eq. 2) expressed in mm/s, should be compared to the 1σ requirement limits that are computed as shown in Equations 3-6.⁷

$$1\sigma_{PointingME} = 17.5 + 0.0035 \times |\bar{V}_C| \quad (3)$$

$$1\sigma_{MagnitudeME} = 10.0 + 0.002 \times |\bar{V}_C| \quad (4)$$

$$1\sigma_{PointingRCS} = 3.5 + 0.02 \times |\bar{V}_C| \quad (5)$$

$$1\sigma_{MagnitudeRCS} = 3.5 + 0.012 \times |\bar{V}_C| \quad (6)$$

The maneuver magnitude errors are typically expressed either as a ΔV magnitude (with units of mm/s) or as a percent of the total maneuver magnitude, though both values are still based on the same computed $\bar{e}_{Magnitude}$ vector. Similarly, while the maneuver pointing error can be expressed as a ΔV in mm/s (which is the magnitude of $\bar{e}_{Pointing}$) this is not geometrically intuitive. Instead it is common for the pointing error to be expressed as the angular separation between the \bar{V}_C and \bar{V}_A (commanded and achieved) burn vectors.

A. Execution Errors of Main Engine Maneuvers

For all 183 Main Engine maneuvers executed by Cassini over the 20-year mission, the execution magnitude error and pointing error terms were computed, as shown in Eq. 1 and 2, and the computed execution error values are shown in Figure 10. As with previous figures, a color-mapping is used to show how the execution errors evolved over the course of the mission (with cooler shades being the earlier maneuvers of the mission and warmer shades being the most recent maneuvers of the mission). On the left-hand plots of Figure 10 the 1σ error bounds defined in Eq. 3 and Eq. 4 are shown as dashed black lines. Recall that the Gates execution error bounds are computed with a linear equation (Eq. 3-6) and the only reason that the black dashed lines in Figure 10 appear to curve is because of the log or semi-log scale used for the plotting axes. Note that for the Cassini ME maneuvers, the pointing error magnitude (upper left plot of Figure 10) shows that the vast majority of the maneuvers had execution errors that were well below the 1σ error bound. In fact, only two maneuvers early in the mission exceeded 1σ in error. The upper-most outlier in the pointing error magnitude plot (upper left plot) corresponds to the Deep Space Maneuver (DSM or TCM-005).

As previously described by Burk⁵, after the execution of the DSM, the Navigation team reported from their radiometric Doppler data that there was a pointing error of ~ 15 mrad, whereas a review of the AACS telemetry of the spacecraft attitude showed that the attitude error of the spacecraft over the course of the maneuver should have resulted in a pointing error of ~ 1.5 mrad. After a thorough review, the SCO team concluded that the most likely explanation for the discrepancy was a mechanical misalignment of the entire Main Engine mounting platform of 15.7 mrad (0.9 degrees). There were several ways that this error could be corrected in the maneuver planning process⁵, and the strategy used by the AACS team was to slew, or “offset”, the spacecraft 15.7 mrad from the computed ΔV direction so that the true ME engine nozzle pointing was properly aligned with inertial ΔV direction. This offset occurred 3 minutes before burn ignition and was used for all ME maneuvers following the DSM (TCM-005). Pointing errors for all later ME maneuvers

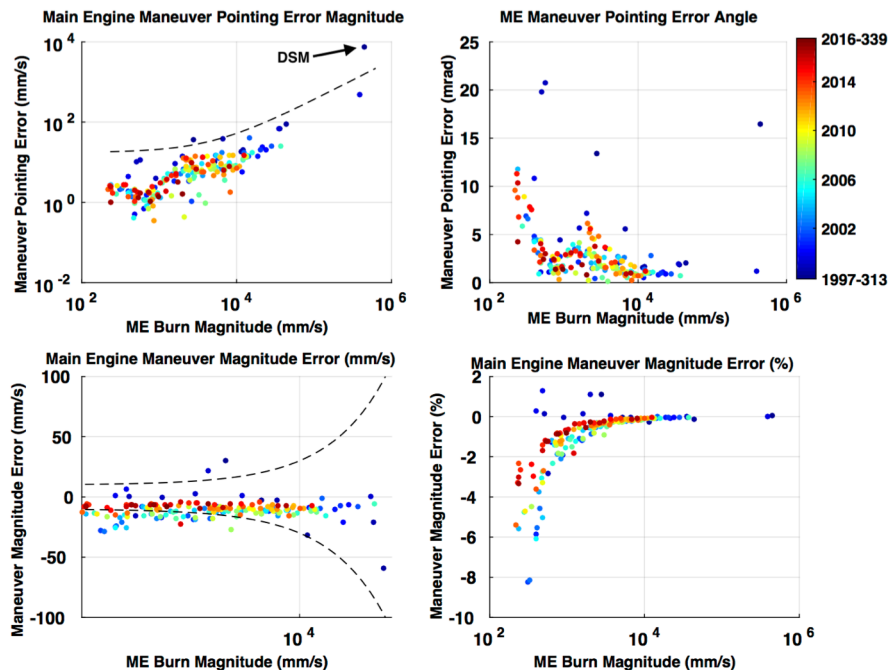


Figure 10. Cassini Main Engine maneuver execution errors. The measured maneuver execution pointing errors, expressed in mm/s and as an angle, are shown in the top two plots. The maneuver execution magnitude error, expressed in mm/s and %, are shown in the bottom plots. The left-hand plots include the 1-sigma execution error requirement bounds as dashed black lines

were reduced by the expected amount.

One omitted data point from the execution error plots in Figure 10 is the Saturn Orbit Insertion (SOI) burn. SOI was the largest maneuver of the mission but, unlike the other maneuvers that were pointed in a fixed inertial direction, the SOI burn was actually an energy burn (ΔE)^{7,12} that targeted a final Keplerian orbital energy level relative to Saturn and the burn direction actually rotated across an arc of 46 degrees relative to the J2000 inertial reference frame.⁷ This rotation tracked the motion of Cassini’s velocity vector with respect to Saturn. As a result of the non-inertial burn direction for the SOI burn, the Gates execution

error terms cannot be computed in the same manner, and so SOI is neglected from the reporting of execution errors in this paper.

An examination of the ME maneuver magnitude error (bottom left and bottom right plots in Figure 10) shows that the ME maneuvers magnitude errors *appear* to consistently fall in the negative region. A negative maneuver magnitude error corresponds to an “under-burn” whereas a positive magnitude error would be an “over-burn.” It is important to stress that the apparent under-burns shown in the bottom left of Figure 10 are not representative of the true maneuver performance.^{13,14} Additional elaboration on this point is required: For all Cassini maneuvers, the NAV team was ultimately responsible for estimating the total achieved maneuver burn size and execution errors. The AACS team recognized the superior accuracy of the Navigation team’s burn reconstruction, and maneuver performance was tailored based on their reported burn execution errors. Over the course of the mission it was observed that while the AACS telemetry commonly showed an apparent under-burn (Figure 10), the more accurate NAV Doppler reconstruction would show that the ME execution error magnitude was well within requirements.¹³ The AACS team did not attempt to remove the apparent under-burns reported by the AACS telemetry because the Navigation reconstruction was the “truth” value that the Flight System performance was calibrated around.

The AACS Flight Software parameters and maneuver sequences were actively updated over the course of the mission to ensure that maneuver execution error magnitudes were minimized to the greatest extent practical. During the course of the mission, the maneuver execution error magnitudes were kept small in two ways: first, scale factor parameter updates for the single axis accelerometer were sent to the AACS FSW. Scale factor updates were especially important in limiting the execution error magnitudes of the large main engine maneuvers. Second, the AACS FSW also carried a parametric value for the amount of ΔV that was imparted by the main engine after the ME latch valve had shut, but while the remaining bipropellant in the thrust chamber was still venting. This “tail-off” impulse was relatively insignificant for large main engine maneuvers, but could be a relatively large fraction of the total ΔV for small ME maneuvers. The AACS team believes that an idiosyncrasy of the AACS FSW for Main Engine ΔV control meant that the tail-off ΔV was not properly included in the ΔV that was reported in the AACS telemetry. It was this idiosyncrasy that the AACS team believes was the source of the apparent under-burns in Figure 10, but it is again emphasized that these apparent under-burns are an artifact of the AACS telemetry. As previously reported in other Cassini maneuver publications, the true Cassini Main Engine maneuver execution performance was remarkably accurate throughout the mission.

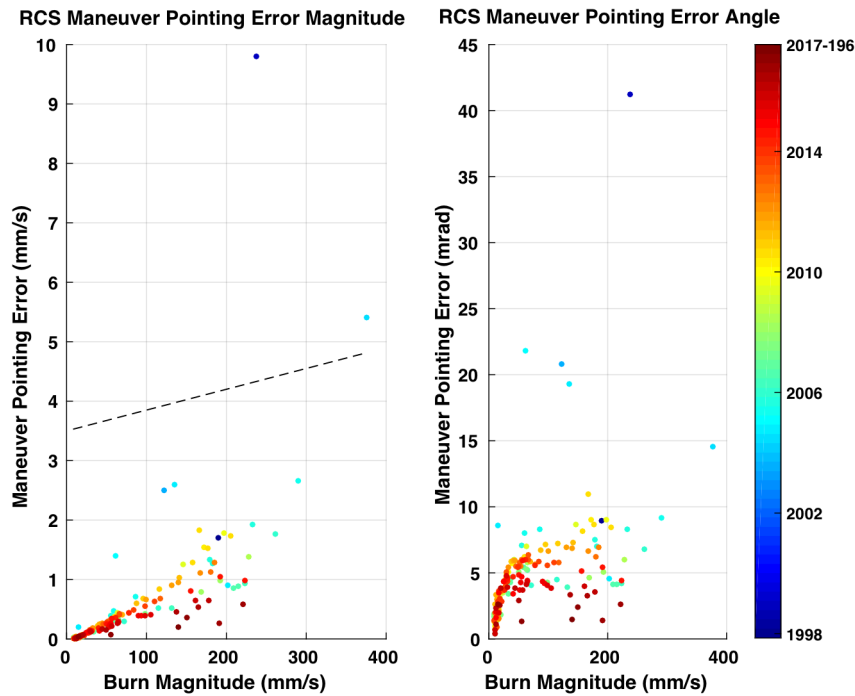


Figure 11. Cassini RCS maneuver execution errors. *The measured RCS maneuver execution pointing error, expressed in mm/s and as an angle are shown. The 1-sigma execution error requirement bound is visible on the left. The color-mapping shows the evolution of the pointing error performance over time.*

B. Execution Errors of RCS Maneuvers

For all 177 RCS maneuvers executed by Cassini over the 20-year mission, the maneuver pointing error was computed, as shown in Eq. 2 and the achieved pointing error values are shown in Figure 11. Again, the color-mapping is used in Figure 11 to show how the execution errors evolved over the course of the mission. Note that unlike the ME maneuvers in Section VII.A., the AACS team does not report any maneuver *magnitude* error values for the RCS maneuvers. Magnitude errors for the RCS maneuvers have no value because the maneuver cutoff for RCS burns was determined based on RCS on-time accumulation instead by an accelerometer. Since the RCS maneuvers were effectively “timed burns,” it naturally followed that the AACS telemetry would show that the

magnitude of the RCS maneuver would be nearly exactly what was commanded. Since AACS lacked an independent sensor to detect the magnitude errors, the AACS team instead left it to the Navigation team to report the maneuver magnitude errors for RCS maneuvers.

Despite the inability of the AACS subsystem to make a meaningful estimate of the RCS maneuver magnitude error, the AACS attitude estimation telemetry could be used to make accurate estimates of the attitude error over the course of the burn. The AACS team therefore focused on the maneuver pointing errors computed for the RCS maneuvers and these values are the ones shown in Figure 11.

The maneuver pointing errors shown in Figure 11 are expressed as a ΔV magnitude in mm/s on the left and as an angular separation (between \bar{V}_C and \bar{V}_A) on the right. The left-hand plot of Figure 11 includes a dashed black line that shows the 1σ error requirement for the RCS maneuvers. Clearly the vast majority of the RCS maneuvers fell well below the requirement limit, with the only exceptions being the first RCS maneuver TCM-002 (which was an uncalibrated maneuver), and OTM-004, which happened to be the longest RCS maneuver of the mission at 464 seconds. Note that in Figure 11 there is a temporal trend in the sizes of the pointing error. During the later years of the Cassini mission, the RCS maneuver pointing error values continued to decrease and this can be seen by examining some of the darkest shades of red that fall at values that are substantially lower than the blue, green, and yellow dots that resulted from earlier maneuvers of a comparable duration. The primary reason for the gradual improvement in RCS maneuver pointing error accuracy was logic in the Cassini FSW that automatically adjusted the off-pulse duration to attempt to decrease the total number of RCS on/off cycles and to minimize pointing error. The ΔV off-pulse adjustment logic was self-learning and improved gradually as more data from past RCS maneuvers was accumulated. The impact of this off-pulse adjustment logic will be discussed in the next section.

VIII. Maneuver Attitude Control Error

As discussed in Section VII, maneuver pointing error is a key measure of maneuver execution quality. The maneuver execution error is definitely affected by spacecraft attitude knowledge error, thruster or engine misalignments, several other small error terms. However, by far the largest contribution to the maneuver pointing error comes from the spacecraft attitude control error during maneuvers. Maneuvers are inherently dynamic events

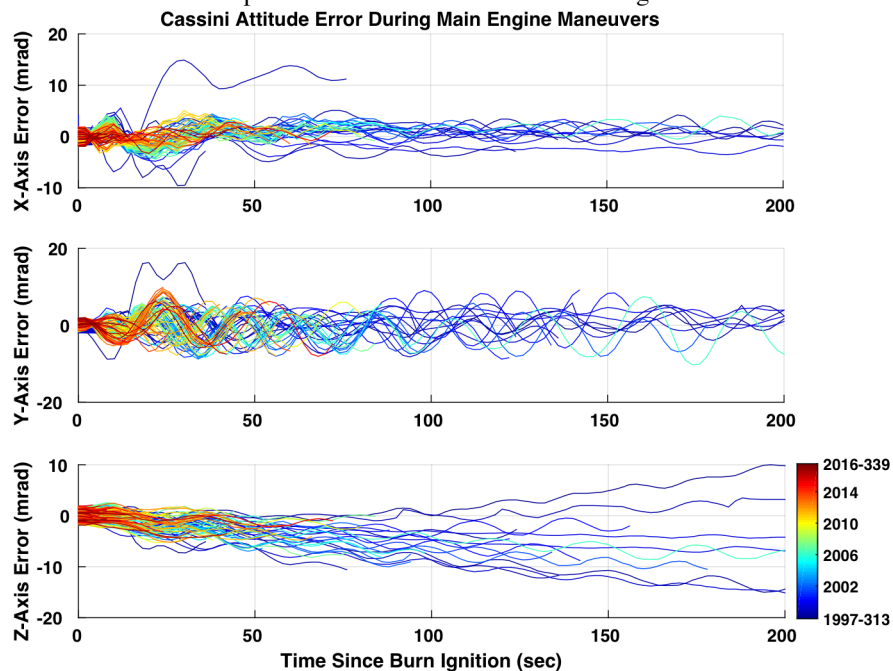


Figure 12. Cassini attitude error during Main Engine maneuvers. *The attitude control error relative to the X, Y, and Z axes of the SC body frame are shown during the first 200 seconds of all main engine maneuvers. The ignition transients in the X and Y axes during the first 30 second of the maneuver are visible, as is the persistent 30-second period oscillation in the Y-axis telemetry. This plot does not show the data beyond 200 seconds for the longest main engine maneuvers.*

that induce significant disturbances into the spacecraft attitude error and rate error. The ability of the ΔV controller logic to minimize the attitude error during maneuvers directly impacts the magnitude of the maneuver pointing error. For this reason, it is worth reviewing more closely the performance of the attitude controller during both the ME and RCS maneuvers.

A. Attitude Control Errors During Main Engine Maneuvers

For Main Engine maneuvers, the X and Y attitude errors were controlled during the burns with the two-axis gimbal on the Main Engine. Z-axis control for the ME burns was performed using the Y-facing RCS thruster couples. The X and Y axis attitude error was linearly

controlled, so the ME gimbal attempted to actively hold the errors at 0 mrad. However, for the Z-axis, the RCS controller included position error deadbands of 17.5 mrad (1.0 deg). Since the Main Engine produced force primarily along the Z-axis, there was very little rotational disturbance around the Z-axis, and so the Y-facing thrusters only needed to pulse infrequently to keep the Z-axis attitude error within +/-1 degree of the commanded burn attitude.

The attitude control measured around the X, Y, and Z axes of the spacecraft body frame during Main Engine maneuvers is shown in Figure 12. The plots in Figure 12 cut off after 200 seconds, so the behavior during the longest ME maneuvers is not visible, but the attitude error during the first 3 minutes is representative of what is seen later in the longer maneuvers. For the vast majority of ME maneuvers the X-axis attitude error experiences an ignition transient that grew to +/-5 mrad before settling out to a value that typically was no more than about +/-3 mrad. The Y-axis attitude error typically saw the largest startup transients with attitude error often oscillating between +/-10 mrad. Also visible to keen-eyed observers in the Y-axis attitude error is the 25-30 s (0.03-0.04 Hz) oscillation previously discussed in Section VI.⁷ This 30 second oscillation never damps out, even for the longest maneuvers. During the 97 min SOI burn, 88 min DSM, and 51 min OTM-002 (PRM) the 30 second oscillation signature is evident in the AACCS attitude error telemetry for the entirety of the burn.

The Z-axis attitude error in Figure 12 appears to be slowly growing in an unbounded manner, but recall that the deadband limit was +/-17.5 mrad, so the Z-axis error never grew large enough to warrant controller activity during the 200 seconds that are plotted. For longer maneuvers the Z-axis error is seen to “bounce” off the deadband limit when pairs of Y-thrusters fire for Z-axis control.

The color-mapping of the plotted lines in Figure 12 show how the attitude error evolved over the mission, but there were no clear temporal trends in the data. The main driver in the size of the position error transients following burn ignition was the accuracy of the ME-A preaim pointing used prior to ignition. Ideally, if the ME-A preaim vector was perfect, then the ME-A nozzle would provide thrust exactly through the SC center of mass and no X and Y axis attitude transient would be observed. Imperfect ME-A preaim pointing would result in large growth in the X and Y axis attitude error early in the maneuver that would be reduced over the course of the longer burns. The history of the preaim vector setting was shown previously in Figure 9. Large attitude transients following burn ignition were typically taken as a cue to the AACCS team that it was time to update the ME-A preaim vector.

B. Attitude Control Errors During RCS Maneuvers

During RCS maneuvers, attitude control is performed entirely with the RCS thrusters. The Z-axis attitude error was controlled, as usual, with the Y-facing thruster couples. X and Y axis attitude error was controlled with the Z-facing thrusters. However, during RCS maneuvers all four Z-facing thrusters turn on simultaneously and then X and Y attitude error was controlled by briefly off-pulsing pairs of Z-facing thrusters.^{6,8} The RCS ΔV controller design maintained the attitude errors within position deadband limits. For all RCS maneuvers the deadband settings were +/-8.7 mrad (0.5 deg) for the X and Y axes, and +/-17.5 mrad (1.0 deg) for the Z-axis.⁵

As previously discussed, in 2009 Cassini swapped from the A-branch of RCS thrusters that had been used from 1997-2009 to the B-branch of RCS thrusters that were used exclusively from 2009-2017.¹⁰ The RCS thruster branch swap was necessitated by the apparent degradation of two of the Z-facing thrusters in the A-branch.⁹ Although the A-branch and B-branch thrusters are co-aligned and were co-located as closely as possible (e.g. Z2A was mounted as closely to Z2B as was practical), the A-branch and B-branch thrusters nevertheless do have different effective lever arms. As a result, the attitude control error telemetry for RCS maneuvers was distinctly different for the A-branch than it was for the B-branch, and so the telemetry from those thruster branches will be discussed separately.

Figure 13 shows the attitude control error for all three spacecraft body axes during the RCS maneuvers that occurred on the A-branch of thrusters. Observe that for the earliest RCS maneuvers (purple, blue, green, and yellow shades) the X and Y axis attitude errors tended to go straight to the 8.7 mrad deadband limit (+8.7 mrad in the case of the X-axis and -8.7 mrad for the Y-axis) and stay there for the remainder of the maneuver. Since the attitude error was continuously at the deadband limit after the first ~15 seconds of the maneuver, it is not surprising that the maneuver pointing error values seen for the pre-2006 maneuvers shown earlier in Figure 11 were commonly in the 7-10 mrad range for long RCS maneuvers, and were even larger for the short RCS maneuvers.

An additional observation about the Y-axis attitude error in Figure 13 is the change in polarity of the attitude error following the release of the Huygens probe. Prior to the probe release, the Y-axis attitude error during the A-branch RCS maneuvers always drifted immediately towards the -8.7 mrad deadband limit. However, after the 320 kg Huygens probe was released from the -X side of spacecraft, the spacecraft center of mass location flipped from the +X to the -X side of the spacecraft YZ plane, and so the Y-axis torque from the four firing RCS thrusters changed direction and the attitude error polarity switched from -Y to +Y.

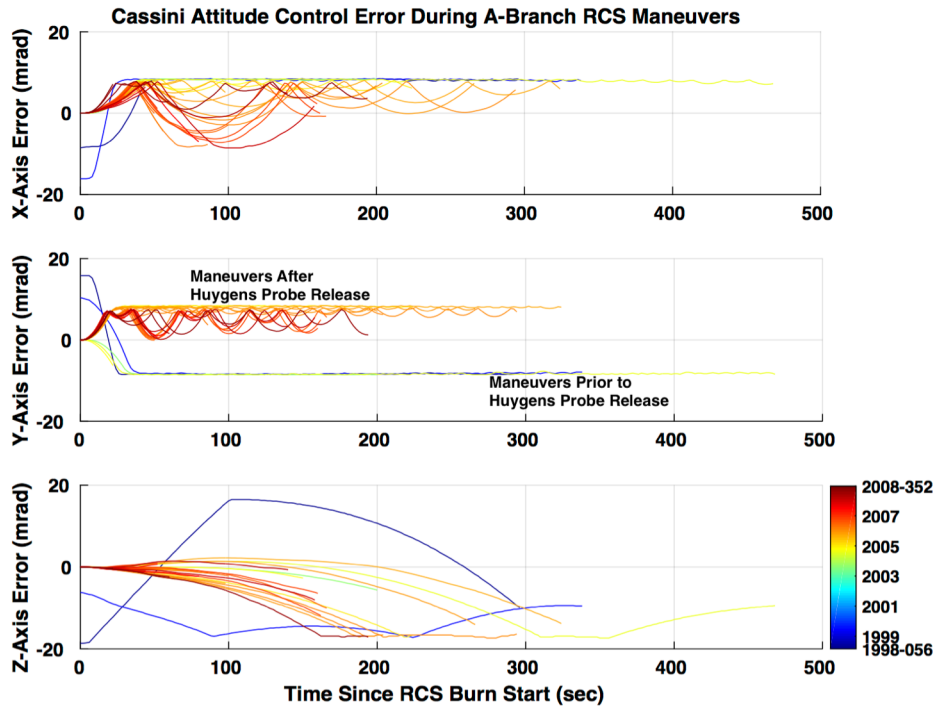


Figure 13. Cassini A-branch RCS maneuver attitude error. *The attitude control error relative to the X, Y, and Z axes of the SC body frame are shown for all RCS maneuvers executed on the A-branch RCS thrusters. The swap in polarity of the Y-axis attitude error in 2005 occurred after the release of the Huygens probe.*

To encourage longer periods between off-pulses and larger parabolic “bounces” of the attitude error between encounters with the deadband limit, the RCS ΔV controller included an attitude integrator (also called a summer) which autonomously learned the ideal off-pulse duration to use based on the attitude error performance during the accumulated active time in the RCS ΔV control mode. The self-learning correction to the RCS ΔV controller did an excellent job at gradually improving RCS maneuver performance, but one complaint of the AACCS operations team is that it took the integrator far too long to “learn” the proper behavior. An inspection of the data plotted in Figure 13 shows that the RCS ΔV attitude error doesn’t begin to show the desirable off-pulse “bounces” away from the deadband until ~2006-2007, which was already 10 years into the mission. Granted that there were significant mass properties changes several times during that period which interfered with the “learning” process, but nevertheless, a superior design would have only needed a small number of long RCS maneuvers to learn from.

After performing 48 RCS maneuvers on the A-branch of thrusters, in 2009 Cassini swapped to the B-branch of thrusters and the B-branch was used for the remaining 129 RCS maneuvers. The attitude control error around the SC X, Y, and Z axes for those 129 RCS maneuvers that occurred between 2009 and 2017 is shown in Figure 14. By the time the spacecraft transitioned to the B-branch thrusters, all of the major mass-shedding events (e.g. probe release, and major ME maneuvers) had already been completed. And so, the B-branch controlled RCS maneuvers show a much more clean and continuous evolution over time. The reader will observe in all three axes of Figure 14 that the size of the parabolic “bounces” away from the deadband limits grows progressively as the data goes from earlier (cold/blue shades) to more recent (warm/red) shades. By the end of the mission, the X and Y attitude errors for the B-branch RCS maneuvers were “bouncing” well past the zero-line and were approaching the opposite deadband limit. The dark red shaded curves in Figure 14 show that the last (i.e. most recent) RCS maneuvers of the mission had the smallest pointing error because they spent more time (on average) near the zero line. These most recent RCS maneuvers had markedly better pointing error performance than maneuvers of similar duration that occurred earlier in the mission (blue and green shades). The gradual improvement in attitude control error shown in Figure 14 is believed to be primarily due to the center of mass shifting, as the bipropellant and monopropellant were consumed, in a favorable direction that had better balanced Z-thruster lever arms.

Note that there is one outlier curve in Figure 14 (in blue) that begins at a position error value that is non-zero and then proceeds to chatter exactly at the deadband limit in both the X and Y axes, though it is only easily visible for the Y-axis telemetry. This outlier case was OTM-265 that occurred in 2010. Shortly before that maneuver occurred, the AACCS team was performing Flight Software maintenance on the Attitude Control Flight Computers (AFCs) which

The final noteworthy observation about the X and Y attitude error telemetry in Figure 13 is the gradually improving off-pulsing behavior in the later maneuvers (the orange, red, and dark red shades). It is undesirable for the attitude error to remain exactly at the deadband limit. Doing so results in “chattering,” that quickly accumulates a large number of thruster on/off cycles. Additionally, remaining at the deadband limit means that the average pointing error value tends to approach the deadband limit setting. It is far more desirable for the RCS off-pulses during the maneuver to force the attitude error to “bounce” further from the deadband limit and, ideally, all the way back towards or across the zero-error line.

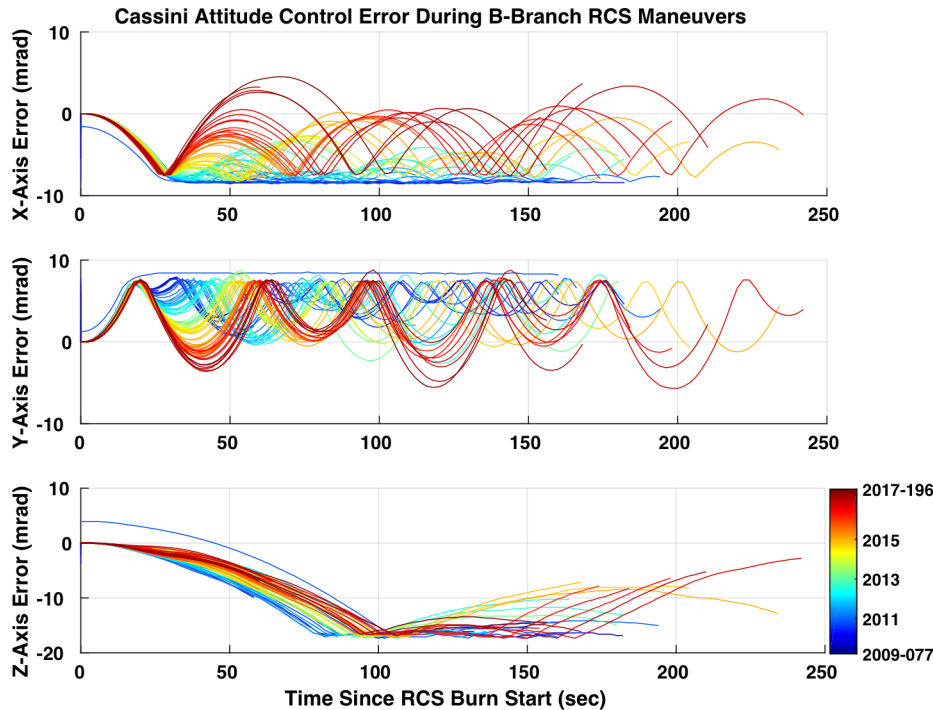


Figure 14. Cassini B-branch RCS maneuver attitude error. *The attitude control error relative to the X, Y, and Z axes of the SC body frame are shown for all RCS maneuvers executed on the B-branch RCS thrusters. The X and Y attitude errors shows a desirable trend of increasingly long periods between thruster off-pulses as the mission progressed.*

control following the safing when it came time to execute OTM-265, the attitude error at the start of the maneuver was much larger than would typically be the case if the slews to the maneuver attitude had been performed using RCS control. After the spacecraft was fully restored after the safing event and after the execution of OTM-265, the AACS team did ultimately perform a direct memory patch to the RCS integrator variables so that all RCS OTMs after late 2010 benefitted from the “self-learning” that had been accomplished during the prior 13 years of the mission.

IX. Conclusion

In the early morning hours of Sept 15, 2017, the Cassini operations teams gathered in the control room at JPL to watch the last telemetry from Cassini as the spacecraft plunged into the atmosphere of Saturn and was destroyed. The Plunge into Saturn capped a phenomenally successful science mission that spanned two decades. Following the intentional destruction of the spacecraft, the Cassini operations team has now switched our focus to documentation and data archiving. Since the large number of executed maneuvers for Cassini was unique among spacecraft built at JPL, the AACS team felt that it was important to try to document as much detail about the AACS performance during the ΔV maneuvers while the team was still intact and the knowledge base was still active.

The results shown in this paper are an example of how the AACS performance during Cassini’s ΔV maneuvers typically outperformed the execution error requirements by a wide margin. This was achieved by the fusion of a well-designed ΔV control logic in the Cassini AACS FSW, as well as the ground process used to design, build, and test the maneuver sequences. The maneuver planning process was a well-developed and well-thought-out process that successfully identified and corrected errors during the planning process so that mistakes were not uplinked to the spacecraft. The Cassini ground tool used to build the maneuver command sequence was continually updated and debugged over the course of the mission so that it continued to produce error-free maneuver sequences. Additionally, the ΔV controller logic in the Cassini FSW was robust and performed excellently across the many years of flight.

After spending 8 years as part of the Cassini AACS team and witnessing the recent destruction of the spacecraft, to write this paper was its own catharsis. However, writing a paper that summarized events that occurred across a time range of 20 years presented its own challenges. By 2017, the Cassini AACS team had developed ground tools that would automatically process the telemetry from ΔV maneuvers and produce reports of the maneuver performance

involved resetting and swapping from the prime to the backup computers. The reset, swap, and loading of the new FSW version worked as expected, but as a result of the FSW reset the “self-learning” RCS off-pulse adjustment logic was reset to its uninitialized state and thus began anew the process of learning the ideal off-pulse behavior from scratch. The AACS team anticipated this, and could have sent direct memory patch commands to restore the RCS integrator values to their pre-FSW reset values. However, an unanticipated spacecraft safing event transitioned the spacecraft to RCS control and the safing recovery activities took priority over the timely restoration of the RCS attitude integrator memory patch activity. Since the spacecraft was still on RCS

and execution errors. As I slowly worked my way backward in time, accumulating telemetry from progressively older maneuvers, the challenges of this analysis continued to mount. For example, maneuvers older than one date would cause scripts to crash due to subtle differences in telemetry collection. Querying telemetry for maneuvers older than a different date needed a special manual process due to flight software changes that occurred early in the mission. Additionally, a great deal of effort by many teams went into the planning and design of each maneuver. The presentations and output files produced by the various subsystems during the OTM planning process were vital parts of understanding the context and idiosyncrasies of each maneuver. However, as I continued to plumb deeper and deeper into the seemingly bottomless well of Cassini data, the maneuver planning products that I was accustomed to using were less reliably available and ultimately ceased to exist (because they had not yet been developed for the earliest maneuvers). Papers could be (and certainly are) written solely on the topic of how data should be maintained on projects with such a long duration. In the end, many of my questions about the earliest Cassini maneuvers were answered in the informative Cassini AACS AIAA papers^{5,7} that were published shortly after Cassini arrived at Saturn 12 years ago.

X. Appendix

The following table includes the relevant vital statistics for all 360 executed maneuvers of the Cassini mission. The maneuver execution magnitude error is not included for RCS maneuvers since the RCS maneuvers were effectively timed burns (i.e. did not use an accelerometer to sense acceleration). The average RCS duty cycle is included for the RCS maneuvers but is not applicable to ME maneuvers. The execution error values for the SOI maneuver are not included because this maneuver was not at a fixed burn direction. Due to the length of time that has elapsed since the earliest years of the mission, some details related to the planning of the early maneuvers (TCM-001 through OTM-009) were not readily available for fresh analysis. For that reason, the “Vc” values were drawn from the NAV team’s data archive, the “Va” values from AACS telemetry, and the execution errors for these maneuvers were taken from the values previously published by Burk⁵.

The limited space of the column header precluded more descriptive names, so they are included here:

- Vc: Commanded ΔV vector magnitude
- Va: Achieved ΔV vector magnitude
- E_{Mag}: Maneuver execution magnitude error
- E_{Angle}: Angular separation between Vc and Va (i.e. pointing error angle)
- E_{Point}: Maneuver execution pointing error
- Avg. DC: Average Duty Cycle during RCS maneuver
- RA: Right Ascension of the maneuver ΔV vector
- DEC: Declination of the maneuver ΔV vector

Maneuver Name	Burn Ignition Time	Burn Type	Vc (m/s)	Va (m/s)	Burn Duration (s)	E _{Mag} (mm/s)	E _{Angle} (mrad)	E _{Point} (mm/s)	Avg. DC (%)	RA (Deg)	DEC (deg)
TCM-001	1997-313T20:00	ME	2.746	2.753	34.5	29.9	13.4	36.9	--	279.8	24.3
TCM-002	1998-056T20:15	RCS	0.185	0.189	292.0	--	8.9	1.7	91.6	164.0	26.6
TCM-005	1998-337T06:00	ME	449.974	449.668	5255.0	256.6	16.4	7399.1	--	3.9	-2.8
TCM-006	1999-035T20:00	ME	11.551	11.545	120.1	32.0	1.6	18.0	--	305.1	-10.8
TCM-007	1999-138T17:10	RCS	0.239	0.238	335.5	--	41.2	9.8	91.4	258.4	-8.7
TCM-009	1999-187T17:00	ME	43.544	43.551	459.5	59.0	2.0	87.6	--	265.3	44.1
TCM-010	1999-200T16:00	ME	5.133	5.127	54.6	2.7	2.0	10.1	--	274.8	66.1
TCM-011	1999-214T21:30	ME	36.309	36.301	391.4	21.2	1.9	67.2	--	62.3	15.3
TCM-012	1999-223T15:30	ME	12.256	12.253	133.4	10.4	1.6	19.9	--	293.3	76.5
TCM-013	1999-243T16:00	ME	6.710	6.706	72.2	2.6	5.6	37.5	--	76.4	24.3
TCM-014	2000-166T17:00	ME	0.555	0.562	6.0	15.6	20.8	11.5	--	18.8	47.2
TCM-017	2001-059T17:30	ME	0.512	0.504	5.3	0.7	19.8	10.5	--	264.8	-63.6
TCM-018	2002-093T18:00	ME	0.901	0.895	9.7	0.5	4.5	4.0	--	195.3	61.5
TCM-019	2003-121T20:00	ME	1.598	1.601	17.4	2.4	5.7	9.1	--	47.0	21.6
TCM-019a	2003-253T19:52	RCS	0.120	0.122	197.6	--	20.8	2.5	92.2	108.0	22.1
TCM-019b	2003-275T04:00	ME	2.000	2.021	39.3	22.0	7.2	14.4	--	29.0	3.3
TCM-020	2004-148T22:26	ME	34.723	34.724	362.0	0.5	2.0	68.3	--	238.8	28.2
TCM-021	2004-168T21:07	ME	3.696	3.685	38.3	1.2	3.5	13.1	--	275.3	-15.4
SOI	2004-183T01:12	ME	625.616	611.773	5818.8	--	--	--	--	271.9	4.2

OTM-002	2004-236T15:53	ME	392.941	393.472	3067.8	100.4	1.2	481.0	--	292.7	9.9
OTM-003	2004-251T16:30	ME	0.495	0.482	3.5	6.4	1.1	0.5	--	183.4	-73.7
OTM-004	2004-297T06:00	RCS	0.372	0.376	464.4	--	14.5	5.4	91.6	80.2	26.4
OTM-005	2004-303T06:15	ME	0.639	0.630	4.6	8.2	1.1	0.7	--	160.0	-8.4
OTM-006	2004-326T05:00	ME	0.407	0.396	3.0	1.1	10.8	4.5	--	141.2	1.3
OTM-008	2004-352T01:22	ME	11.903	11.896	84.8	8.9	0.5	5.9	--	299.3	-78.6
OTM-009	2004-358T00:52	RCS	0.016	0.015	18.6	--	8.6	0.2	97.2	16.7	-10.8
OTM-010	2004-363T00:37	ME	23.759	23.753	153.3	6.2	0.9	20.6	--	200.0	7.8
OTM-010a	2005-003T23:38	RCS	0.135	0.135	147.4	--	19.3	2.6	92.6	71.9	45.9
OTM-011	2005-016T09:20	ME	21.583	21.563	140.2	20.7	1.1	23.6	--	320.8	2.5
OTM-012	2005-028T07:08	ME	18.661	18.650	120.0	10.4	0.8	14.4	--	305.6	-0.5
OTM-013	2005-043T06:07	RCS	0.203	0.202	220.3	--	4.6	0.9	92.4	59.4	21.5
OTM-014	2005-049T06:00	ME	0.693	0.683	4.5	9.4	2.3	1.6	--	20.1	-6.2
OTM-015	2005-061T04:50	ME	6.233	6.226	40.0	7.2	1.3	8.0	--	238.9	73.8
OTM-017	2005-071T03:20	ME	0.419	0.395	2.7	24.6	4.9	1.9	--	232.9	26.7
OTM-018	2005-078T18:19	ME	1.587	1.568	10.3	18.5	2.1	3.3	--	258.2	-74.2
OTM-020	2005-094T02:22	ME	0.901	0.884	5.8	17.4	2.7	2.4	--	49.7	-30.5
OTM-021	2005-100T02:00	ME	5.833	5.821	37.4	12.0	2.1	12.4	--	314.4	-71.7
OTM-022	2005-104T02:40	RCS	0.060	0.061	67.4	--	21.8	1.4	92.2	313.6	-24.1
OTM-024	2005-119T00:58	ME	20.533	20.525	131.5	7.6	1.0	20.4	--	338.6	-71.5
OTM-025	2005-189T20:37	ME	0.336	0.308	2.1	27.7	6.9	2.1	--	246.3	-5.1
OTM-026	2005-215T11:50	ME	2.602	2.589	16.6	12.3	0.4	1.0	--	37.7	20.5
OTM-027	2005-222T13:21	ME	2.392	2.384	15.4	7.9	1.5	3.5	--	152.3	-57.7
OTM-029	2005-237T17:08	ME	1.433	1.418	9.2	15.5	3.5	5.0	--	74.0	-44.3
OTM-030	2005-242T18:43	ME	14.323	14.314	91.4	9.3	1.0	14.0	--	166.5	-57.1
OTM-031	2005-246T17:30	RCS	0.059	0.059	66.6	--	8.0	0.5	91.3	109.1	11.7
OTM-033	2005-262T16:40	ME	27.888	27.879	176.2	8.2	0.9	25.3	--	105.6	36.2
OTM-035	2005-271T16:11	RCS	0.290	0.290	321.0	--	9.2	2.7	92.5	28.2	-5.6
OTM-038	2005-285T05:57	ME	14.783	14.782	92.7	1.3	2.8	41.2	--	13.0	-10.3
OTM-039	2005-294T14:58	RCS	0.086	0.086	96.4	--	8.3	0.7	92.1	223.2	-7.3
OTM-041	2005-304T13:59	ME	12.382	12.371	77.6	11.1	1.4	17.6	--	22.7	-3.6
OTM-042	2005-317T14:02	ME	2.087	2.068	13.2	18.3	3.3	6.9	--	322.7	7.7
OTM-043	2005-327T13:03	RCS	0.055	0.056	62.9	--	7.0	0.4	92.7	248.3	11.3
OTM-044	2005-332T04:15	RCS	0.232	0.233	262.5	--	8.3	1.9	93.2	4.7	-19.0
OTM-047	2005-364T02:47	RCS	0.179	0.179	198.6	--	7.5	1.3	93.0	64.8	67.2
OTM-051	2006-033T07:53	RCS	0.182	0.182	203.0	--	7.0	1.3	93.1	56.3	-28.6
OTM-053	2006-061T05:51	RCS	0.261	0.261	291.4	--	6.8	1.8	92.9	234.7	24.7
OTM-056	2006-081T04:19	ME	0.428	0.404	2.7	23.7	4.4	1.8	--	268.3	4.2
OTM-057	2006-096T03:32	ME	0.355	0.326	2.2	28.9	6.7	2.2	--	126.9	-1.0
OTM-058	2006-117T01:59	RCS	0.071	0.072	53.0	--	4.1	0.3	92.2	70.3	-4.5
OTM-059	2006-124T01:28	ME	0.465	0.444	3.0	21.4	3.1	1.4	--	313.5	21.8
OTM-061	2006-138T00:41	RCS	0.114	0.115	85.0	--	4.5	0.5	91.9	170.2	4.3
OTM-063	2006-158T23:24	ME	1.900	1.890	12.0	9.9	2.8	5.3	--	60.6	41.5
OTM-064	2006-179T22:07	RCS	0.064	0.064	47.6	--	4.2	0.3	91.6	221.5	26.0
OTM-065	2006-186T21:36	RCS	0.132	0.132	96.9	--	3.9	0.5	92.8	134.4	39.4
OTM-069	2006-213T20:05	ME	5.393	5.382	33.8	11.4	2.7	14.6	--	352.2	61.3
OTM-070	2006-247T18:21	RCS	0.223	0.223	164.1	--	4.2	0.9	92.3	148.6	15.8
OTM-071	2006-253T18:00	ME	6.534	6.522	40.9	12.1	2.6	17.1	--	335.8	20.3
OTM-072	2006-257T10:07	ME	8.134	8.124	50.8	10.8	1.1	9.0	--	332.9	56.2
OTM-075	2006-274T09:08	ME	6.449	6.438	40.3	10.5	1.0	6.7	--	26.2	48.5
OTM-076	2006-279T16:24	RCS	0.036	0.036	26.5	--	4.5	0.2	94.3	143.3	33.7
OTM-078	2006-290T15:40	ME	0.839	0.821	5.2	17.6	1.6	1.3	--	92.3	45.2
OTM-079	2006-295T15:26	RCS	0.058	0.058	44.3	--	5.4	0.3	90.5	137.6	31.3
OTM-080	2006-313T14:28	ME	3.632	3.620	22.7	11.7	1.3	4.7	--	318.9	-24.9
JTM-081	2006-331T13:15	RCS	0.215	0.215	160.1	--	4.1	0.9	93.0	123.9	44.3
OTM-083	2006-349T12:03	ME	0.762	0.748	4.8	14.3	1.4	1.0	--	6.0	-6.4
OTM-084	2006-354T11:48	ME	6.831	6.816	42.7	15.5	0.9	6.0	--	342.3	-1.2
OTM-086	2006-365T11:05	ME	0.449	0.433	2.8	16.8	4.5	1.9	--	346.8	-18.3
OTM-087	2007-005T10:50	ME	1.626	1.608	10.2	18.4	3.2	5.1	--	334.5	-20.2

OTM-088	2007-010T10:20	RCS	0.037	0.037	27.6	--	4.6	0.2	94.4	317.4	-31.4
OTM-089	2007-016T02:36	RCS	0.208	0.209	158.5	--	4.1	0.9	92.5	327.7	-41.9
OTM-090	2007-021T09:36	ME	2.351	2.339	14.7	12.4	2.0	4.7	--	318.7	-32.2
OTM-091	2007-026T09:21	RCS	0.010	0.011	7.6	--	0.4	0.0	100.1	117.6	33.4
OTM-093	2007-038T08:37	ME	0.252	0.238	1.5	14.1	11.8	2.8	--	222.6	-43.6
OTM-094	2007-050T07:37	RCS	0.037	0.037	28.0	--	4.3	0.2	94.2	231.9	-34.0
OTM-096	2007-061T06:51	ME	0.647	0.639	4.1	7.7	1.9	1.2	--	176.9	-2.9
OTM-098	2007-072T06:06	ME	1.057	1.046	6.6	11.6	1.2	1.3	--	97.2	38.9
OTM-099	2007-077T05:50	ME	1.596	1.585	10.0	10.8	3.7	5.8	--	202.8	-4.1
OTM-100	2007-081T20:30	RCS	0.064	0.064	49.8	--	5.2	0.3	92.8	135.4	-37.1
OTM-101	2007-087T20:49	ME	0.509	0.483	3.2	25.7	4.5	2.2	--	78.8	38.3
OTM-102	2007-093T04:34	ME	2.680	2.667	16.7	12.8	2.1	5.6	--	202.0	9.4
OTM-103	2007-097T20:48	RCS	0.033	0.033	25.9	--	3.4	0.1	93.7	151.1	-10.7
OTM-105	2007-109T03:32	ME	3.520	3.508	21.9	11.7	2.6	9.2	--	190.6	46.2
OTM-106	2007-114T03:16	RCS	0.012	0.012	8.9	--	2.3	0.0	100.0	196.1	24.0
OTM-108	2007-124T19:00	ME	5.563	5.551	34.5	12.2	2.6	14.6	--	201.1	61.6
OTM-109	2007-129T02:14	RCS	0.019	0.021	14.5	--	1.8	0.0	95.8	262.8	-29.5
OTM-111	2007-141T01:27	ME	5.527	5.515	34.3	11.4	1.4	7.5	--	202.4	61.9
OTM-113	2007-152T00:41	ME	0.688	0.678	4.3	9.7	1.2	0.8	--	23.1	1.2
OTM-114	2007-156T16:55	ME	12.228	12.218	75.6	9.8	0.9	11.2	--	227.5	72.8
OTM-115	2007-162T00:10	RCS	0.032	0.033	25.5	--	4.4	0.1	93.6	161.3	62.6
OTM-116	2007-167T23:39	ME	0.741	0.731	4.6	10.5	1.5	1.1	--	328.6	26.3
OTM-117	2007-172T23:23	ME	7.959	7.948	49.0	11.3	1.2	9.8	--	323.8	84.1
OTM-118	2007-177T23:08	RCS	0.009	0.009	6.9	--	1.9	0.0	100.0	150.3	-4.3
OTM-119	2007-184T22:37	RCS	0.018	0.019	13.9	--	1.8	0.0	98.3	121.0	-30.1
OTM-121	2007-196T22:06	RCS	0.009	0.009	7.0	--	1.7	0.0	100.0	62.0	-2.4
JTM-123	2007-218T20:35	ME	0.422	0.397	2.6	25.6	4.3	1.7	--	198.3	7.8
OTM-125	2007-245T11:35	ME	0.480	0.465	3.0	14.7	0.9	0.4	--	159.1	39.1
OTM-128	2007-256T18:20	ME	13.472	13.461	83.4	10.3	1.1	14.9	--	311.7	65.1
OTM-129	2007-260T18:21	RCS	0.098	0.099	79.0	--	4.3	0.4	92.2	65.0	-46.0
OTM-130	2007-271T17:36	RCS	0.019	0.020	14.4	--	1.9	0.0	96.7	289.1	64.5
OTM-131	2007-278T17:22	ME	1.319	1.303	8.2	16.3	4.0	5.1	--	301.8	35.3
OTM-132	2007-305T15:40	ME	0.970	0.955	6.0	15.2	1.8	1.7	--	276.3	-49.0
OTM-133	2007-319T14:56	RCS	0.062	0.063	50.8	--	5.3	0.3	91.0	245.0	-4.6
OTM-134	2007-326T06:57	ME	1.159	1.148	7.2	11.5	3.4	3.9	--	352.5	34.2
OTM-135	2007-331T06:43	ME	15.753	15.737	96.5	16.0	1.1	17.4	--	281.9	62.6
OTM-136	2007-336T13:44	RCS	0.014	0.014	10.6	--	1.4	0.0	100.0	188.6	16.1
OTM-137	2007-342T06:00	ME	0.672	0.657	4.2	15.6	1.7	1.1	--	193.5	12.0
OTM-138	2007-347T07:10	ME	9.633	9.620	59.1	13.4	0.8	8.4	--	254.2	74.3
OTM-139	2007-352T05:16	RCS	0.009	0.009	7.1	--	1.8	0.0	100.0	131.0	55.3
OTM-141	2007-363T12:02	ME	2.044	2.032	12.6	12.3	3.1	6.2	--	193.2	68.0
OTM-143	2008-016T04:15	ME	2.873	2.861	17.6	11.8	1.5	4.4	--	129.4	-1.7
OTM-144	2008-037T02:06	ME	37.388	37.383	227.9	5.8	0.7	25.7	--	215.0	35.5
OTM-145	2008-050T08:36	ME	0.289	0.275	1.7	13.7	5.8	1.6	--	64.3	36.8
OTM-146	2008-061T22:56	ME	7.018	7.005	42.6	12.8	0.5	3.5	--	225.7	-44.7
OTM-147	2008-067T07:21	ME	1.111	1.098	6.8	12.7	2.8	3.1	--	338.5	74.3
OTM-149	2008-073T23:21	ME	2.753	2.742	16.7	10.6	1.5	4.0	--	166.6	24.0
OTM-150	2008-078T06:35	RCS	0.049	0.050	40.5	--	5.0	0.3	91.7	192.2	-38.7
OTM-152	2008-102T01:04	ME	3.315	3.299	20.2	16.6	0.5	1.6	--	345.9	21.6
OTM-153	2008-117T03:47	ME	0.499	0.485	3.1	13.6	2.0	1.0	--	330.8	-34.2
OTM-155	2008-138T01:20	ME	1.163	1.145	7.1	17.7	3.1	3.6	--	339.2	26.2
OTM-156	2008-143T02:13	RCS	0.192	0.192	155.1	--	5.1	1.0	92.8	164.7	-11.7
OTM-159	2008-175T06:24	ME	12.158	12.146	73.5	12.1	1.0	11.8	--	32.9	64.3
OTM-160	2008-209T14:36	RCS	0.168	0.169	139.0	--	4.6	0.8	92.1	238.9	-67.0
OTM-162	2008-216T22:15	ME	2.528	2.518	15.4	10.5	3.0	7.6	--	336.0	44.1
OTM-164	2008-236T02:49	ME	13.518	13.506	81.2	12.6	1.0	13.1	--	83.4	68.2
OTM-164a	2008-264T18:49	ME	0.883	0.866	5.3	16.7	1.7	1.4	--	62.2	52.2
OTM-165	2008-276T10:19	ME	3.923	3.912	23.7	11.2	0.1	1.0	--	104.7	66.9
OTM-166	2008-280T18:05	RCS	0.010	0.010	8.1	--	1.8	0.0	100.0	186.6	2.3

OTM-167	2008-286T23:51	ME	3.329	3.317	20.0	12.1	1.7	5.7	--	228.9	-72.4
OTM-168	2008-291T09:10	ME	6.984	6.971	41.7	13.4	0.9	6.4	--	127.2	40.3
OTM-169	2008-303T16:37	RCS	0.228	0.228	191.0	--	6.0	1.4	91.4	167.8	-45.8
OTM-170	2008-313T22:23	ME	9.091	9.076	54.6	15.2	0.9	7.9	--	207.9	-61.2
OTM-171	2008-317T22:09	ME	5.142	5.128	30.9	14.1	1.3	6.6	--	337.8	28.6
OTM-173	2008-328T21:25	ME	0.774	0.759	4.7	14.0	1.6	1.2	--	331.4	18.1
OTM-175	2008-336T20:56	RCS	0.064	0.064	57.5	--	5.8	0.4	89.3	301.8	-35.0
OTM-176	2008-344T20:27	ME	3.029	3.002	18.2	27.2	2.0	5.9	--	108.4	54.6
OTM-177	2008-348T20:13	ME	1.616	1.599	9.7	17.4	4.1	6.6	--	36.2	58.0
OTM-178	2008-352T19:58	RCS	0.022	0.023	19.6	--	3.5	0.1	90.5	148.9	-10.2
OTM-180	2009-024T03:48	ME	4.663	4.650	27.8	13.3	1.5	6.9	--	95.9	52.7
OTM-182	2009-041T10:04	ME	0.360	0.344	2.1	16.1	7.7	2.7	--	93.4	1.5
OTM-183	2009-068T08:20	ME	5.017	5.004	29.9	12.5	1.7	8.6	--	220.0	-46.0
OTM-183x	2009-077T00:05	RCS	0.016	0.016	12.8	--	1.7	0.0	100.0	129.7	19.6
OTM-186	2009-088T13:05	ME	0.745	0.735	4.4	10.6	1.0	0.7	--	138.2	13.9
OTM-189	2009-102T12:04	ME	7.119	7.107	42.2	12.5	1.1	8.0	--	103.1	49.1
OTM-192	2009-118T11:02	ME	2.482	2.475	14.8	7.7	1.5	3.7	--	124.5	27.9
OTM-195	2009-134T10:00	ME	2.217	2.199	13.2	17.8	3.0	6.6	--	287.6	-33.2
OTM-196	2009-138T19:45	RCS	0.042	0.042	37.6	--	6.0	0.3	88.2	268.8	-44.7
OTM-198	2009-150T08:58	ME	1.455	1.447	8.7	8.2	1.0	1.5	--	330.5	16.2
OTM-200	2009-161T08:12	ME	2.135	2.126	12.7	8.9	0.2	0.4	--	263.6	-58.8
OTM-201	2009-166T01:26	RCS	0.025	0.025	22.0	--	3.9	0.1	91.5	238.9	-49.2
OTM-203	2009-177T07:09	ME	2.413	2.403	14.3	9.9	2.7	6.4	--	273.3	-30.4
OTM-204	2009-182T00:24	RCS	0.011	0.011	9.1	--	1.2	0.0	100.0	235.0	-43.9
OTM-206	2009-193T16:22	ME	3.506	3.497	20.8	8.8	1.8	6.2	--	290.4	-3.6
OTM-207	2009-198T15:52	RCS	0.027	0.028	24.1	--	4.5	0.1	92.2	268.2	-35.1
OTM-209	2009-209T15:21	ME	6.283	6.271	37.1	11.8	1.4	8.9	--	301.3	22.9
OTM-210	2009-213T22:35	RCS	0.017	0.018	14.8	--	3.1	0.1	94.4	258.2	-20.9
OTM-213	2009-228T14:04	ME	12.990	12.979	76.5	10.6	1.1	14.2	--	335.3	60.8
OTM-215	2009-241T13:19	ME	0.502	0.486	3.0	16.5	4.4	2.1	--	293.8	44.2
OTM-216	2009-248T02:48	ME	4.469	4.459	26.3	10.4	1.7	7.7	--	300.3	66.5
OTM-217	2009-282T11:04	RCS	0.145	0.146	130.1	--	8.6	1.3	89.0	281.1	-0.5
OTM-218	2009-289T00:34	ME	0.842	0.834	5.0	8.0	2.5	2.1	--	222.4	65.7
OTM-219	2009-294T00:04	ME	4.157	4.148	24.4	9.5	3.4	14.3	--	22.4	68.1
OTM-220	2009-302T23:35	RCS	0.063	0.063	56.8	--	7.0	0.4	90.2	306.5	0.9
OTM-221	2009-309T09:20	ME	0.303	0.289	1.7	14.3	8.9	2.6	--	243.7	-10.2
OTM-224	2009-326T22:22	ME	2.546	2.535	14.9	10.3	4.6	11.6	--	89.2	-7.5
OTM-225	2009-338T07:39	RCS	0.197	0.197	180.4	--	9.0	1.8	89.1	146.6	-5.0
OTM-227	2009-349T06:55	ME	0.709	0.700	4.2	9.1	2.7	1.9	--	100.5	-14.0
OTM-228	2009-354T06:41	ME	2.219	2.207	13.1	12.5	3.5	7.8	--	339.3	-66.0
OTM-231	2010-005T05:43	ME	8.037	8.027	47.1	10.4	1.9	15.1	--	48.9	45.5
OTM-232	2010-009T19:29	RCS	0.031	0.031	28.4	--	4.7	0.1	90.5	181.7	12.1
OTM-233	2010-016T04:59	ME	2.259	2.248	13.3	11.1	5.7	12.8	--	89.6	30.6
OTM-234	2010-021T04:45	ME	6.060	6.052	35.5	7.7	2.2	13.5	--	50.0	51.3
OTM-236	2010-032T04:01	ME	6.196	6.167	36.2	10.6	2.2	13.6	--	202.5	12.0
OTM-237	2010-054T16:33	RCS	0.010	0.010	8.8	--	1.0	0.0	100.0	260.7	-50.7
OTM-240	2010-085T14:19	ME	2.990	2.981	17.5	9.2	2.5	7.6	--	64.4	-56.9
OTM-241	2010-092T13:49	RCS	0.029	0.030	26.6	--	4.9	0.1	91.3	112.1	26.3
OTM-242	2010-100T23:19	ME	9.031	9.024	52.7	7.4	1.6	14.9	--	271.9	-85.0
OTM-243	2010-108T12:33	RCS	0.040	0.040	38.3	--	5.7	0.2	91.4	113.5	-3.0
OTM-245	2010-119T11:47	ME	5.704	5.696	33.3	7.9	1.0	5.8	--	93.2	-8.7
OTM-246	2010-131T11:01	ME	8.873	8.864	51.5	8.8	0.7	6.5	--	40.7	68.0
OTM-248	2010-143T10:15	ME	0.843	0.831	4.9	11.3	1.0	0.8	--	106.8	-33.7
OTM-249	2010-148T09:44	ME	10.757	10.747	62.4	9.4	0.7	8.0	--	82.3	-82.9
OTM-250	2010-152T19:44	RCS	0.032	0.032	29.3	--	5.1	0.2	90.1	162.4	9.6
OTM-252	2010-164T08:42	ME	1.228	1.207	7.2	7.5	2.9	3.5	--	11.8	71.4
OTM-253	2010-169T02:11	RCS	0.020	0.020	18.9	--	3.6	0.1	89.1	165.0	10.4
OTM-254	2010-175T07:56	ME	0.863	0.852	5.0	10.3	0.4	0.3	--	57.2	50.8
OTM-255	2010-181T07:40	ME	6.247	6.223	36.2	6.9	1.5	9.5	--	57.5	58.6

OTM-256	2010-185T01:09	RCS	0.017	0.017	14.6	--	2.3	0.0	97.0	181.9	11.4
OTM-257	2010-191T06:53	ME	0.826	0.816	4.8	10.0	1.5	1.2	--	297.1	-16.3
OTM-258	2010-199T06:37	ME	6.760	6.749	39.1	10.6	0.7	4.9	--	198.7	-88.0
OTM-261	2010-246T03:33	ME	2.431	2.421	14.1	10.1	4.6	11.2	--	222.9	22.0
OTM-261a	2010-259T02:47	RCS	0.172	0.172	158.8	--	9.0	1.5	89.0	307.1	5.1
OTM-264	2010-288T01:02	RCS	0.177	0.177	165.1	--	8.6	1.5	88.4	190.7	7.0
OTM-265	2010-312T09:48	RCS	0.166	0.167	157.5	--	11.0	1.8	87.9	182.0	7.4
OTM-267	2010-325T23:05	ME	2.240	2.231	13.1	9.4	5.2	11.7	--	231.9	-73.9
OTM-268	2010-331T16:20	RCS	0.060	0.060	55.9	--	6.2	0.4	89.3	149.2	29.0
JTM-269	2010-335T22:21	RCS	0.158	0.158	146.9	--	8.2	1.3	88.5	234.3	-20.3
OTM-270	2010-342T22:07	RCS	0.011	0.011	9.5	--	0.8	0.0	100.0	73.2	-10.5
OTM-273	2011-001T06:40	RCS	0.205	0.205	191.3	--	8.4	1.7	89.0	113.9	-40.7
OTM-274	2011-008T06:26	RCS	0.029	0.030	27.9	--	4.7	0.1	89.7	131.2	-72.4
OTM-275	2011-014T13:27	ME	2.755	2.746	16.0	8.7	2.7	7.5	--	82.8	71.2
OTM-276	2011-032T04:44	RCS	0.015	0.016	13.1	--	1.7	0.0	97.7	185.5	65.1
OTM-279	2011-061T10:17	RCS	0.095	0.096	89.3	--	7.2	0.7	89.5	166.3	64.2
OTM-280	2011-105T23:48	RCS	0.015	0.016	13.1	--	1.5	0.0	98.2	347.0	2.5
OTM-281	2011-112T06:48	RCS	0.038	0.038	35.5	--	5.8	0.2	88.7	293.8	43.4
OTM-283	2011-125T22:17	RCS	0.009	0.009	8.1	--	1.3	0.0	100.0	314.9	3.8
OTM-284	2011-132T05:32	RCS	0.116	0.116	109.4	--	7.2	0.8	89.5	173.4	-8.3
OTM-285	2011-144T04:46	RCS	0.032	0.032	30.0	--	4.4	0.1	90.0	8.9	6.4
OTM-286	2011-168T02:57	RCS	0.010	0.010	8.8	--	2.7	0.0	100.0	313.9	-3.3
OTM-287	2011-175T08:42	RCS	0.141	0.141	133.6	--	7.3	1.0	88.4	205.8	3.5
OTM-288	2011-234T15:04	RCS	0.088	0.088	83.8	--	6.8	0.6	88.6	340.4	-3.1
OTM-291	2011-263T03:17	ME	5.045	5.036	29.4	9.4	0.9	4.8	--	193.4	-70.9
OTM-292	2011-271T13:02	RCS	0.028	0.028	26.8	--	4.4	0.1	89.0	104.7	-1.9
OTM-294	2011-278T02:17	RCS	0.070	0.070	66.1	--	5.8	0.4	89.3	66.2	-15.4
OTM-297	2011-301T11:17	RCS	0.041	0.041	40.3	--	6.0	0.2	87.0	58.5	-13.4
OTM-299	2011-313T00:17	ME	2.077	2.067	12.0	9.5	6.2	12.8	--	91.3	-55.6
OTM-300	2011-328T05:18	ME	2.962	2.952	17.2	9.5	4.8	14.2	--	345.1	5.9
OTM-300a	2011-335T23:04	RCS	0.016	0.017	13.8	--	2.1	0.0	93.7	251.0	6.6
OTM-301	2011-343T08:49	RCS	0.013	0.013	11.3	--	3.0	0.0	100.0	130.2	-67.5
OTM-303	2011-351T08:20	ME	0.503	0.489	2.9	13.6	2.9	1.4	--	261.2	48.3
OTM-304	2011-356T21:51	RCS	0.011	0.012	10.1	--	3.3	0.0	100.0	245.4	13.4
OTM-306	2012-016T06:39	RCS	0.044	0.044	44.1	--	5.9	0.3	85.7	155.3	58.9
OTM-308	2012-034T05:27	RCS	0.131	0.131	124.4	--	6.9	0.9	89.1	214.1	28.2
JTM-310	2012-048T04:29	RCS	0.015	0.015	12.9	--	2.2	0.0	99.0	270.3	8.2
OTM-312	2012-070T03:01	ME	3.567	3.553	20.6	14.6	1.6	5.7	--	181.0	16.1
OTM-312a	2012-076T02:46	RCS	0.100	0.100	95.6	--	6.7	0.7	88.8	249.6	4.2
OTM-313	2012-084T16:02	RCS	0.011	0.011	10.0	--	1.6	0.0	100.0	259.8	4.9
OTM-314	2012-091T01:32	RCS	0.140	0.140	133.8	--	6.8	1.0	88.4	31.1	54.5
OTM-316	2012-102T14:48	RCS	0.026	0.027	25.5	--	3.9	0.1	88.8	257.0	5.4
OTM-318	2012-115T07:33	ME	0.233	0.220	1.3	12.6	9.6	2.1	--	336.7	39.4
OTM-319	2012-120T07:17	RCS	0.030	0.030	29.5	--	4.7	0.1	88.3	283.4	5.6
OTM-321	2012-135T06:01	ME	8.262	8.246	47.6	15.6	0.2	1.8	--	333.2	-83.1
JTM-322	2012-140T22:16	RCS	0.077	0.078	73.5	--	5.7	0.4	89.0	201.7	-20.8
OTM-324	2012-151T05:00	ME	3.704	3.696	21.4	8.2	1.6	5.8	--	260.7	-73.2
OTM-325	2012-155T21:15	RCS	0.033	0.033	31.8	--	5.4	0.2	89.0	155.8	-9.4
OTM-326	2012-162T10:29	ME	0.412	0.397	2.4	14.8	3.4	1.4	--	272.0	16.7
OTM-327	2012-173T03:28	ME	10.109	10.100	58.0	9.4	0.7	7.0	--	262.4	-64.3
OTM-328	2012-203T07:38	RCS	0.167	0.167	161.3	--	6.6	1.1	88.6	175.3	-12.8
OTM-330	2012-220T06:36	ME	4.342	4.336	25.0	6.2	2.1	9.0	--	265.5	-31.9
OTM-331	2012-267T13:47	RCS	0.055	0.056	55.8	--	6.0	0.3	87.7	14.6	31.2
OTM-332	2012-274T03:16	RCS	0.184	0.185	179.0	--	6.9	1.3	89.6	328.0	18.1
OTM-333	2012-283T13:01	ME	0.747	0.741	4.3	6.0	2.3	1.7	--	53.8	15.7
OTM-334	2012-314T18:46	RCS	0.054	0.054	55.5	--	5.5	0.3	86.1	210.7	-5.1
OTM-335	2012-322T00:31	ME	0.245	0.239	1.4	5.7	8.8	2.1	--	207.9	-65.6
OTM-336	2012-327T00:16	ME	4.951	4.947	28.4	4.2	2.2	10.7	--	251.6	-14.1
OTM-337	2012-331T00:01	RCS	0.016	0.016	15.1	--	1.6	0.0	96.3	337.6	-45.4

OTM-338	2012-337T23:32	RCS	0.022	0.022	22.5	--	3.6	0.1	87.5	228.0	-47.5
OTM-339	2013-030T20:09	ME	1.648	1.643	9.5	5.0	2.8	4.6	--	269.7	33.5
OTM-340	2013-044T05:26	RCS	0.026	0.027	27.4	--	4.4	0.1	86.3	218.5	-30.3
OTM-341	2013-055T12:12	ME	1.441	1.436	8.3	5.1	3.3	4.7	--	257.3	36.5
OTM-342	2013-061T04:28	ME	0.254	0.247	1.5	6.8	6.9	1.7	--	87.6	-72.7
OTM-345	2013-076T03:29	RCS	0.180	0.180	177.5	--	6.2	1.1	89.1	274.5	19.5
OTM-346	2013-091T16:16	RCS	0.011	0.011	10.0	--	2.0	0.0	100.0	51.8	45.3
OTM-347	2013-099T01:46	RCS	0.117	0.117	115.9	--	5.8	0.7	89.2	54.6	51.7
OTM-348	2013-120T08:02	ME	0.486	0.479	2.8	6.8	2.2	1.0	--	249.4	11.7
OTM-349	2013-139T12:46	RCS	0.011	0.011	10.3	--	0.8	0.0	100.0	44.4	59.3
OTM-350	2013-147T06:01	RCS	0.045	0.046	44.9	--	5.5	0.3	89.3	45.0	18.7
OTM-351	2013-162T21:14	ME	0.809	0.803	4.7	6.7	3.0	2.4	--	109.2	-52.7
OTM-352	2013-188T09:26	RCS	0.052	0.052	53.8	--	5.8	0.3	86.6	70.2	-42.8
JTM-353	2013-196T02:40	ME	0.239	0.231	1.4	7.8	11.3	2.6	--	43.7	21.2
OTM-354	2013-200T02:25	ME	2.255	2.248	12.9	6.8	5.6	12.6	--	106.6	-49.9
OTM-355	2013-204T08:24	RCS	0.066	0.067	66.9	--	6.0	0.4	89.4	280.1	50.3
OTM-357	2013-219T07:22	ME	3.604	3.598	20.6	5.4	3.6	13.1	--	288.5	53.1
OTM-358	2013-252T05:18	RCS	0.029	0.029	30.3	--	5.1	0.1	86.4	152.0	-32.9
OTM-359	2013-259T04:47	RCS	0.027	0.027	28.6	--	4.0	0.1	86.5	43.6	20.8
OTM-360	2013-273T04:01	RCS	0.066	0.066	66.0	--	6.4	0.4	89.3	124.0	-22.7
OTM-361	2013-284T03:15	RCS	0.013	0.013	11.9	--	0.9	0.0	100.0	125.3	-49.7
OTM-363	2013-306T12:15	ME	0.352	0.343	2.0	8.4	7.9	2.7	--	331.5	50.6
OTM-364	2013-332T00:45	RCS	0.008	0.008	7.8	--	1.4	0.0	100.0	209.9	-42.2
OTM-366	2013-351T23:32	ME	0.376	0.365	2.1	11.2	7.5	2.7	--	321.3	55.6
OTM-367	2013-363T22:48	RCS	0.110	0.110	110.0	--	5.8	0.6	89.8	327.5	48.8
OTM-368	2014-005T16:03	RCS	0.098	0.098	99.4	--	5.6	0.5	88.4	194.6	-37.5
OTM-370	2014-030T20:51	RCS	0.050	0.050	51.0	--	5.5	0.3	88.7	330.2	48.8
OTM-371	2014-036T14:07	RCS	0.083	0.084	85.6	--	5.8	0.5	88.1	202.4	21.1
OTM-372	2014-048T13:24	ME	1.669	1.664	9.6	5.1	3.0	5.1	--	13.6	25.7
OTM-373	2014-062T18:56	RCS	0.018	0.018	19.8	--	3.1	0.1	86.1	344.4	33.9
OTM-375	2014-079T11:28	ME	0.528	0.522	3.0	6.2	3.5	1.8	--	22.0	8.3
OTM-376	2014-094T10:29	RCS	0.049	0.049	50.5	--	5.4	0.3	88.5	193.7	-29.6
OTM-377	2014-101T10:00	RCS	0.032	0.032	33.4	--	4.4	0.1	87.1	105.8	-6.5
OTM-378	2014-114T09:01	RCS	0.030	0.031	32.4	--	4.6	0.1	86.7	54.2	-2.9
OTM-379	2014-134T07:46	RCS	0.017	0.017	17.3	--	3.6	0.1	91.7	142.3	56.7
OTM-380	2014-141T07:16	RCS	0.014	0.014	13.4	--	2.8	0.0	100.0	152.0	31.1
OTM-382	2014-166T11:44	RCS	0.021	0.022	23.0	--	2.8	0.1	87.0	259.5	35.9
OTM-383	2014-173T04:59	RCS	0.040	0.040	41.3	--	4.7	0.2	89.5	256.8	8.9
OTM-385	2014-198T09:40	RCS	0.026	0.027	29.0	--	4.3	0.1	85.1	91.4	-38.3
OTM-387	2014-221T08:08	ME	12.450	12.443	71.0	7.2	1.2	14.5	--	277.6	30.7
OTM-388	2014-230T07:37	RCS	0.027	0.027	29.0	--	3.7	0.1	85.1	172.1	7.4
OTM-390	2014-250T06:19	ME	1.257	1.234	7.2	22.8	1.6	2.0	--	257.7	12.8
OTM-391	2014-262T05:33	RCS	0.078	0.078	78.9	--	5.6	0.4	90.6	257.5	42.3
OTM-392	2014-269T05:02	RCS	0.061	0.061	63.3	--	6.0	0.4	88.2	322.3	28.2
OTM-393	2014-282T04:16	ME	1.050	1.044	6.0	6.6	2.9	3.0	--	71.2	5.1
OTM-394	2014-294T03:30	RCS	0.030	0.030	32.1	--	4.5	0.1	86.2	52.5	-49.0
OTM-395	2014-300T20:44	RCS	0.056	0.057	59.8	--	5.9	0.3	87.1	287.7	48.5
OTM-396	2014-326T01:44	RCS	0.192	0.192	200.6	--	5.5	1.0	87.4	112.1	-7.7
OTM-397	2014-341T18:30	RCS	0.031	0.032	33.8	--	4.5	0.1	86.5	305.0	-47.4
OTM-398	2014-348T00:15	RCS	0.155	0.156	164.4	--	5.2	0.8	86.9	237.4	60.0
OTM-399	2014-363T23:31	ME	0.954	0.947	5.5	6.6	1.7	1.6	--	78.8	27.0
JTM-400	2015-009T22:47	RCS	0.050	0.050	51.3	--	4.8	0.2	89.1	99.3	-51.3
OTM-401	2015-014T22:32	RCS	0.223	0.223	231.5	--	4.4	1.0	88.4	238.1	27.8
OTM-402	2015-031T21:34	ME	1.254	1.249	7.2	4.6	3.1	3.8	--	84.0	47.3
OTM-403	2015-040T21:06	RCS	0.023	0.024	25.4	--	4.3	0.1	86.1	245.3	-23.4
OTM-404	2015-046T20:36	ME	0.489	0.481	2.8	8.2	4.1	2.0	--	251.2	6.8
OTM-405	2015-063T19:39	RCS	0.094	0.094	100.3	--	4.2	0.4	86.9	330.9	7.1
OTM-406	2015-072T19:10	RCS	0.017	0.017	17.6	--	3.5	0.1	91.8	193.9	-21.4
OTM-408	2015-110T16:29	RCS	0.041	0.041	44.0	--	3.4	0.1	88.6	195.4	-1.8

OTM-409	2015-124T15:30	RCS	0.012	0.012	11.9	--	1.6	0.0	100.0	165.0	0.5
OTM-410	2015-131T15:00	RCS	0.055	0.055	60.3	--	4.7	0.3	86.2	69.9	-2.2
OTM-411	2015-159T13:00	RCS	0.054	0.054	58.1	--	4.3	0.2	87.4	165.6	-9.2
OTM-414	2015-177T11:44	RCS	0.065	0.065	70.5	--	4.4	0.3	85.8	184.5	1.6
OTM-416	2015-191T10:58	RCS	0.090	0.090	97.5	--	4.3	0.4	86.3	34.4	-5.1
OTM-417	2015-221T08:54	RCS	0.012	0.012	11.9	--	2.0	0.0	100.0	143.6	-5.6
OTM-419	2015-233T08:07	RCS	0.052	0.052	56.0	--	3.7	0.2	88.1	53.9	-2.9
OTM-421	2015-268T05:48	RCS	0.016	0.017	16.4	--	2.0	0.0	93.4	123.8	-7.5
OTM-422	2015-275T05:17	ME	0.244	0.236	1.4	7.4	10.4	2.5	--	246.7	-17.6
OTM-423	2015-279T05:02	ME	2.617	2.608	14.9	8.4	3.8	9.9	--	220.5	-79.4
OTM-424	2015-284T04:46	RCS	0.029	0.029	32.5	--	4.8	0.1	84.2	158.3	-7.9
OTM-426	2015-293T04:15	RCS	0.065	0.065	69.5	--	4.4	0.3	87.3	105.2	-0.8
OTM-429	2015-309T03:29	RCS	0.105	0.105	112.1	--	3.8	0.4	87.8	319.4	-4.6
OTM-431	2015-320T02:29	RCS	0.098	0.098	105.3	--	4.1	0.4	87.1	220.0	14.2
OTM-435	2015-364T00:00	ME	2.974	2.968	17.0	6.1	2.2	6.6	--	345.3	84.7
OTM-436	2016-012T23:16	RCS	0.030	0.031	34.4	--	3.9	0.1	84.9	192.2	6.5
OTM-438	2016-023T22:47	ME	6.834	6.827	38.7	7.4	0.9	6.2	--	86.8	79.4
JTM-439	2016-029T22:17	RCS	0.010	0.010	9.9	--	0.4	0.0	100.0	266.7	-22.7
OTM-440	2016-034T22:03	ME	0.571	0.564	3.3	7.0	3.0	1.7	--	147.1	-12.1
OTM-441	2016-039T21:49	ME	0.734	0.727	4.2	6.4	2.4	1.8	--	115.7	60.5
OTM-442	2016-044T21:34	RCS	0.009	0.010	9.4	--	0.7	0.0	100.0	34.3	21.0
JTM-443	2016-051T21:05	RCS	0.063	0.063	68.5	--	4.1	0.3	87.5	143.5	-33.6
OTM-444	2016-085T18:55	ME	7.938	7.931	45.0	7.5	1.0	7.7	--	114.1	50.7
OTM-445	2016-092T18:26	RCS	0.057	0.057	62.3	--	3.7	0.2	86.0	257.4	1.5
OTM-446	2016-098T18:11	RCS	0.161	0.162	171.8	--	4.0	0.6	87.6	173.6	-34.0
OTM-447	2016-113T17:13	ME	1.754	1.744	10.0	9.4	1.9	3.3	--	125.7	31.8
JTM-448	2016-125T16:29	RCS	0.011	0.012	11.3	--	2.4	0.0	100.0	347.5	-67.2
OTM-449	2016-130T15:59	ME	0.540	0.533	3.1	6.7	2.4	1.3	--	148.6	-15.9
OTM-450	2016-143T15:00	RCS	0.020	0.021	23.1	--	3.8	0.1	84.9	25.6	27.0
OTM-452	2016-163T13:45	ME	0.245	0.237	1.4	8.2	4.2	1.0	--	301.8	-55.4
OTM-453	2016-199T11:13	ME	2.015	2.010	11.5	5.5	0.8	1.7	--	313.8	9.9
OTM-454	2016-204T10:42	RCS	0.044	0.044	47.9	--	3.9	0.2	88.9	288.5	40.9
OTM-455	2016-210T10:27	RCS	0.178	0.178	194.8	--	3.6	0.6	87.2	44.1	45.6
OTM-456	2016-215T10:11	ME	0.781	0.774	4.5	6.7	1.4	1.1	--	118.3	4.4
JTM-459	2016-233T08:54	RCS	0.050	0.050	53.1	--	2.9	0.1	89.8	233.3	-71.8
OTM-460	2016-267T06:34	RCS	0.019	0.019	21.5	--	2.6	0.0	84.3	43.7	19.0
OTM-462	2016-279T05:48	RCS	0.165	0.165	181.3	--	3.3	0.5	87.0	253.0	-58.9
OTM-463	2016-315T03:29	RCS	0.013	0.013	12.5	--	1.1	0.0	100.0	246.7	-54.6
OTM-464	2016-322T03:14	RCS	0.137	0.137	151.0	--	3.3	0.5	86.7	171.4	-55.9
OTM-467	2016-339T11:58	ME	0.984	0.976	5.6	8.0	1.4	1.4	--	163.5	-55.8
OTM-468	2016-359T00:58	RCS	0.221	0.221	239.3	--	2.7	0.6	87.7	177.7	-15.0
OTM-468a	2017-053T15:49	RCS	0.190	0.191	207.4	--	1.4	0.3	88.1	254.9	-10.3
OTM-469	2017-108T18:12	RCS	0.054	0.055	58.0	--	1.4	0.1	88.0	195.3	-61.7
OTM-470	2017-114T17:52	RCS	0.150	0.150	165.3	--	2.4	0.4	87.7	187.8	33.3
OTM-471	2017-130T16:58	RCS	0.014	0.015	14.3	--	2.6	0.0	93.5	210.1	14.0
OTM-472	2017-196T12:21	RCS	0.139	0.139	153.1	--	1.5	0.2	87.2	270.2	20.6

XI. Acknowledgments

The research described in this paper was carried out at the Jet Propulsion Laboratory, California Institute of Technology, under contract with the National Aeronautics and Space Administration. Copyright 2017 California Institute of Technology. Government sponsorship acknowledged. Reference to any specific commercial product, process, or service by trade name, trademark, manufacturer, or otherwise, does not constitute or imply its endorsement by the United States Government or the Jet Propulsion Laboratory, California Institute of Technology.

The author would like to thank the Cassini AACS team for their hard work over the last two decades that went into planning for the mission and then operating the spacecraft after launch. The data for this paper came from too many AACS engineers (both current members and alumni) to mention individually here, but suffice it to say that the analysis of the 360 Cassini maneuvers has been a team effort and I do not claim individual credit for this work. In

particular I want to thank Tom Burk for his support in querying and understanding some of the oldest maneuvers of the mission and because his 2005 paper⁵ on the topic of Cassini's early maneuvers (from well before I was on the project) remains my best understanding of what transpired during the inner solar system cruise. I also want to thank the efforts of Sean Wagner from the Cassini NAV team for his work to maintain the NAV wiki and its treasure trove of data on the NAV reconstruction of all planned and executed Cassini maneuvers. For some early maneuvers where there were issues with the availability of AACS planning products, the NAV wiki was used as a resource to fill gaps in the AACS data.

As we are now dying days of the Cassini project, I want to thank all of the members of the Cassini SCO team, who have been my friends and compatriots for the last 8 years. It has been an honor to be a part of this outstanding mission.

XII. References

¹Matson, D. L., Spilker, L. J., and Lebreton, J. P., "The Cassini/Huygens Mission to the Saturnian System," *Space Science Review*, Vol. 104, 2002, pp. 1-58.

²Sarani, S., "Attitude Control Configuration for Huygens Probe Release," *Proceedings of the AIAA Guidance, Navigation, and Control Conference*, San Francisco, California, August 15-18, 2005.

³Buffington, B., Strange, N., and Smith, J., "Overview of the Cassini Extended Mission Trajectory," AIAA-2008-6752, *Proceedings of the AIAA Guidance, Navigation, and Control Conference*, Honolulu, Hawaii, August 18-21, 2008.

⁴Smith, J., Buffington, B., "Overview of the Cassini Solstice Mission Trajectory," AAS 09-351, *Advances in the Astronautical Sciences Vol. 135*, Presented at the AAS/AIAA Astrodynamics Specialist Conference, Pittsburgh, Pennsylvania, August 9-13, 2009.

⁵Burk, T. A., "Attitude Control Performance During Cassini Trajectory Correction Maneuvers," AIAA 2005-6270, *Proceedings of the AIAA Guidance, Navigation, and Control Conference*, San Francisco, California, August 15-18, 2005.

⁶Wong, E. C., and Breckenridge, W. G., "An Attitude Control Design for the Cassini Spacecraft," AIAA 1995-3274, *Proceedings of the AIAA Guidance, Navigation, and Control Conference*, Baltimore, Maryland, August 1995.

⁷Lee, A. Y., and Hanover, G., "Cassini Spacecraft Attitude Control System Flight Performance," AIAA 2005-6269, *Proceedings of the AIAA Guidance, Navigation, and Control Conference*, San Francisco, California, August 15-18, 2005.

⁸Enright, P. J., "Attitude Control of the Cassini Spacecraft During Propulsive Maneuvers," Paper AAS 93-552, AAS/AIAA Astrodynamics Specialist Conference, Victoria, B. C., Canada, August 1993.

⁹Mizukami, M., Barber, T. J., Christodoulou, L. N., Guernsey, C. S., and Haney, W. A., "Cassini Spacecraft Reaction Control System Thrusters Flight Experience," JANNAP Propulsion Meeting, Colorado Springs, Colorado, May 2010.

¹⁰Bates, David M., "Cassini Spacecraft In-Flight Swap To Backup Attitude Control Thrusters," AIAA-2010-7559, *Proceedings of the AIAA Guidance, Navigation, and Control Conference*, Toronto, Ontario, Canada, August 2-5, 2010.

¹¹Gates, C. R., "A Simplified Model of Midcourse Maneuver Execution Errors," JPL Technical Report 32-504, Jet Propulsion Laboratory, California Institute of Technology, Pasadena, CA, Oct. 1963.

¹²Lam, D.C., Friberg, K.H., Brown, J.M., and Lee, A.Y., "An Energy Burn Algorithm for Cassini Saturn Orbit Insertion," *Proceedings of the AIAA Guidance, Navigation, and Control Conference*, San Francisco, California, USA, August 15-18, 2005.

¹³Wagner, S., "Maneuver Performance Assessment of the Cassini Spacecraft Through Execution-Error Modeling and Analysis," Paper AAS 14-390, AAS/AIAA *Space Flight Mechanic Meeting*, Santa Fe, 2014.

¹⁴Burn, T.A., "Cassini Orbit Trim Maneuvers at Saturn – Overview of Attitude Control Flight Operations," *Proceedings of the AIAA Guidance, Navigation, and Control Conference*, Portland, Oregon, August, 2011.